Electronic Supplementary Material for

Extinction of herbivorous dinosaurs linked to Early Jurassic global warming event.

D. Pol[1]*, J. Ramezani[2], K. Gomez[1], J. L. Carballido[1], A. Paulina Carabajal[3], O.W.M. Rauhut[4], I. H. Escapa[1], N. R. Cúneo[1]

[1]CONICET, Museo Paleontológico Egidio Feruglio, Trelew 9100, Chubut, Argentina. [2]Department of Earth, Atmospheric and Planetary Sciences, Massachusetts Institute of Technology, Cambridge, MA 02139, USA. [3]Instituto de Investigaciones en Biodiversidad y Medioambiente (CONICET-UNCo), San Carlos de Bariloche 8400, Río Negro, Argentina. [4]Bayerische Staatssammlung für Paläontologie und Geologie, Department for Earth and Environmental Sciences, and GeoBioCenter, Ludwig-Maximilians-University Munich, 80333 Munich, Germany.

Correspondent autor: Diego Pol.
Email: dpol@mef.org.ar

DOI: 10.1098/rspb.2020.2310

This PDF file includes:

Other supplementary materials for this manuscript include the following:

Datasets S1 to S2

Supplementary Text

Locality Data. *Bagualia alba* was found in grey mudstone levels from the base of the Cañadón Asfalto Formation. The fossiliferous locality is in the Bagual canyon, located 5 km south of the Cerro Cóndor town in the Chubut Province, Central Patagonia, Argentina. Approximate geographic coordinates are 43° 27' S and 69° 11' W; more precise geographic location is deposited at the MPEF collection and available upon request.

The holotype was found with the posterior half of skull articulated with the first seven cervical vertebrae. These remains were in close association with multiple cranial and postcranial remains belonging to at least three individuals, a minimum number of specimens based on repeated elements (humerus, scapula). The elements represented in these materials include rostral and mandibular elements, over 20 isolated teeth, presacral, sacral, and caudal vertebrae, haemal arches, elements of the pectoral and pelvic girdle, forelimb, and hindlimb (see below List of Materials). All these elements formed a bonebed of approximately 6 mt wide, 3 mt long, and 60 cm deep. All of the repeated sauropod remains can be referred to *Bagualia alba* and the only non-sauropod remains identified are isolated theropod teeth and a fragmentary theropod dentary.

U-Pb Geochronology.

Sample FF022616-1. This sample comes from a uniform, greenish grey, fine-grained tuff collected from the massive pyroclastic breccia outcrops of the Lonco Trapial Formation exposed along the Chubut Highway 12, approximately 62 km south of the town of Paso del Sapo. This location is ~30 km north of the El Bagual fossil site. The tuff matrix was carefully sampled to avoid the abundant gravel- to boulder-size clasts of the polymictic breccia.

Sample EB041412. The tuffaceous silt/mudstones containing the fossil dinosaur bones (Fig. S1) at the El Bagual site was directly sampled for age determination. The bone bed lies in the predominantly lacustrine strata of the basal Cañadón Asfalto Formation, a short stratigraphic distance above basalt flows assigned to the upper Lonco Trapial Formation (or the Lonco Trapial

– Cañadón Asfalto transition). The uppermost basalt flow displays a well-developed paleosol horizon indicating subaerial exposure preceding the deposition of the Cañadón Asfalto strata.

Sample CA041412-2. This sample was collected from a ~10 cm-thick tuffaceous bed collected from the topmost exposures of the Cañadón Asfalto Formation at Cañadón la Huinco, approximately 7.8 km to the S-SE of the El Bagual site. The tuff occurs in the lacustrine carbonate-rich interval of the formation, stratigraphically ~140 m above the top of the uppermost basalt flow and ~15 below the top of the section. The Cretaceous Chubut Group strata overlie the Cañadón Asfalto Formation with a prominent unconformity at this location.

Analytical procedures. Geochronology samples weighed approximately 5 kg and were analysed by the U-Pb chemical abrasion isotope dilution thermal ionization mass spectrometry (CA-ID-TIMS) method, following the same analytical procedures used previously [S1,S2]. After manual sledging and pulverization in a Shatterbox®, samples were water-washed to remove their fine (<10 μm) particles. A zircon-rich mineral concentrate was obtained using magnetic as well as high-density liquid separation. Final zircon selection was carried out by hand picking under a binocular microscope based on crystal morphology. Preference in zircon selection was given to elongate prismatic zircon with glass (melt) inclusions parallel to their crystallographic “c” axis (figure S1) and no detectable evidence of abrasion or rounding (*see* [S2]).

Selected zircon grains were pre-treated by a chemical abrasion method modified after [S3] to mitigate the effects of radiation-induced Pb loss. The chemical abrasion schedule consisted of thermal annealing of zircon at 900°C for 60 hours, followed by partial dissolution in 27M HF at 210°C for 12 hours. Pre-treated zircons were thoroughly fluxed and rinsed to remove leachates and were spiked with the EARTHTIME ET535 mixed ^{205}Pb–^{233}U–^{235}U tracer [S4,S5] before complete acid digestion and analysis. Isotopic ratios of Pb and U were measured on a VG SECTOR 54 multi-collector mass spectrometer equipped with a Daly ion-counting system at the MIT Isotope Laboratory. Isotopic data reduction, date calculation and propagation of uncertainties

were carried out using computer applications Triploi and ET_redux that utilize the algorithms of [S6,S7]. Complete U–Pb data appear in the supplementary material Data S2.

The sample ages are derived from the weighed mean $^{206}Pb/^{238}U$ date of the youngest population of analyses from each sample after excluding older zircons suspected of being detrital or xenocrystic. Uncertainties in the weighed mean $^{206}Pb/^{238}U$ dates are reported at 95% confidence level and follow the notation ± *X*/*Y*/*Z* Ma, where *X* is the internal (analytical) uncertainty in the absence of all external errors, *Y* incorporates *X* and the U–Pb tracer calibration error, and *Z* includes the latter as well as the U decay constant errors of [S8]. Complete uncertainties (*Z*) must be taken into account for comparison between age data from different isotopic chronometers (e.g., U–Pb versus $^{40}Ar/^{39}Ar$), whereas for comparison between U-Pb ID-TIMS dates obtained using the same isotopic tracer (e.g., results of this study and those of [S1]), the external errors can all be ignored. Results of ID-TIMS analyses are presented Table S1, figure S2, and Dataset S2.

All dates obtained from tuff and tuffaceous sedimentary samples are inherently considered maximum constraints on the ages of deposition. Only when a set of consecutive and mutually resolvable (outside the uncertainty) dates are shown to obey the superposition that they can be interpreted as relevant to the true depositional age. In this case, the comprehensive Jurassic chronostratigraphy of the Cañadón Asfalto Basin based on high-precision U-Pb CA-ID-TIMS geochronology established by Cúneo et al. [S1] provides the necessary stratigraphic context for interpretations of our U-Pb dates as reliable estimates of depositional age.

Results. Five single zircon analyses from sample FF022616-1 overlap within analytical uncertainties and yield without any outliers a weighted mean $^{206}Pb/^{238}U$ date of 180.330 ± 0.068/0.11/0.22 Ma with a MSWD of 0.60 (Table S1 and Fig S2). This date is consistent with the previously determined age envelope of 188.95 - 178.77 Ma for the Lonco Trapial Formation based on U-Pb zircon ages of the bracketing tuff beds [S1] and represent the best estimate for the age of its pyroclastic component.

All 5 analyses from sample EB041412 overlap within analytical uncertainties and result in a weighted mean $^{206}Pb/^{238}U$ date of 179.17 ± 0.12/0.16/0.25 Ma with a MSWD of 1.1. This date is consistent with the established chronostratigraphy of the lower Cañadón Asfalto Formation based on high-precision U-Pb ash bed geochronology [S1], particularly a previously reported weighted mean $^{206}Pb/^{238}U$ date of 178.766 ± 0.092 Ma from a tuff bed from the nearby Cañadón Lahuincó locality, which occurs in between two transitional basalt flows of the Lonco Trapial Formation. The U-Pb date reported here, therefore, serves as a reliable constraint on the age of sediment deposition at El Bagual and of the recovered fossils.

A group of six youngest analyses from sample CA041412-2 defines a statistically coherent cluster with a weighted mean $^{206}Pb/^{238}U$ date of 178.07 ± 0.21/0.25/0.31 Ma and with a MSWD of 1.1. Two older grains (z 4 and z8) are interpreted as detrital zircons. The latter date is consistent with, and adds to, an array of previously reported high-precision U-Pb dates from the Cañadón Asfalto Formation [S1] and confirms that the basaltic volcanism in the basin had already ended by ~178 Ma.

Additional Anatomical Information.

We present here further information on the anatomy of *Bagualia alba*. We first include a discussion of the diagnostic features of the new taxon, which are illustrated by the supplementary figures included here. Subsequently, we include a supplementary description that highlights the main features of the anatomy of the skull, mandibular, and cervical vertebrae of *Bagualia alba*. We emphasize features that are phylogenetically informative or relevant to support the affinities with the derived clade Eusauropoda.

Diagnostic features. *Bagualia alba* is diagnosed by a unique combination of nine characters (including six autapomorphies) that distinguish the new taxon from other early sauropods.

1. *Anterior process on the anteroventral end of the premaxilla and anterodorsal end of the dentary*. The anteroventral end of the premaxilla and anterodorsal end of the dentary bear a pointed ("beak-like") process. This feature is very noticeable in the premaxilla in lateral view (blp in figure S3) and in the dentary in anterior view (blp in figure S7b). The presence of a moderate process on the anterior end of the dentary has been reported in some non-sauropod sauropodomorphs (e.g., *Mussaurus* [S9]) but it is not present in other sauropods and is therefore regarded as an autapomorphy of *Bagualia* given its phylogenetic context. Similarly, the presence of a distinct process in the premaxilla has not been reported in other sauropods. It is interesting to note that these two features are absent in the referred premaxilla (PVL 4076) and dentaries (MACN-CH 933, MPEF-PV 1670) of *Patagosaurus fariasi* found in the upper levels of the Cañadón Asfalto Formation, contributing to distinguish *Bagualia* from other eusauropods known from this unit (note that *Volkheimeria* also comes from this unit but lack cranial remains and is retrieved here as an eusauropod outgroup).

2. Anterior margin of the premaxilla without a marked step. The premaxilla of *Bagualia alba* lacks a distinct step along its anterior margin in lateral view. This is a common feature present in all early sauropods and most immediate outgroups (e.g., *Melanorosaurus* [S10]). This distinct step is present in all early eusauropods that have preserved this region (e.g.,

Shunosaurus, *Spinophorosaurus*, *Omeisaurus*, *Mamenchisaurus*) contrasting with the smooth profile of the anterior margin of the premaxilla of *Bagualia alba* (figure S3). The lack of a distinct step is present in sauropodomorphs that are all placed very distantly from *Bagualia* in all MPTs (e.g., in forms more basal than *Melanorosaurus* and also in two derived clades of neosauropods: diplodocoids and derived titanosaurs). Given the distant position of these taxa all these occurrences are optimised as acquired independently from the condition of *Bagualia*.

3*. Orbital margin of the frontal with a close V-shape pointed medially, resulting in a short contribution to the orbit*. The contribution of the frontal to the orbital margin in *Bagualia* is unique among eusauropods. The orbital margin of the frontal is located between articular facets for the prefrontal and postorbital (om in figure 2*b*). The frontal orbital margin forms a deeply concave notch, and its lateral margin has small indentations (figure S5). The configuration of the frontal is different from those of all other known sauropodomorphs and is regarded as an autapomorphy of *Bagualia alba*.

4. *Supratemporal fenestra about as long as wide*. The supratemporal fenestra of *Bagualia* (figure 2*b*) present an intermediate condition between the anteroposteriorly long fenestra that is present in *Shunosaurus* and most early sauropodomorphs (e.g., *Plateosaurus*, *Mussaurus*, *Melanorosaurus*) and the transversely wider fenestra of all eusauropods more derived than *Shunosaurus* (e.g., *Mamenchisaurus*, *Omeisaurus*, *Jobaria*, *Diplodocus*). The closely related *Nebulasaurus* and *Spinophorosaurus* also shows a supratemporal fenestra wider than long. Although there is variation in the proportions of the supratemporal fenestra that indicates the evolution of this character could be more complex that the categories recognized in the commonly used discrete phylogenetic character, the condition of a subequal length and width present in *Bagualia* is interpreted as an autapomorphic character of the new taxon. A similar overall proportion can be found in some Triassic sauropodomorphs (e.g., *Coloradisaurus*) but these are phylogenetically placed far from *Bagualia* so that their similarity in this feature is interpreted as convergently acquired.

5. *Strongly marked and convex proatlantal facets on the laterodorsal margin of the foramen magnum*. (see atf in figure 2*d* and S6*a*). The exoccipital bears a rough bulge that elevates for approximately one centimeter close to its sutural contact with the supraoccipital at the laterodorsal margin of the foramen magnum. This bulge is present in both exoccipitals of the holotype specimen and correspond with the site for the articulation of the proatlas with the occiput (proatlantal facets). The presence of these facets is not autapomorphic as similar facets are also present in other sauropodomorphs, although details on their morphology in *Bagualia* differ from other taxa. Proatlantal facets have been noted in the basal sauropodomorph *Lufengosaurus* ([S11]: fig. 5) and the basal sauropod *Shunosaurus* (skull cast of ZG65430, [S12]) but the facets in *Bagualia* are much larger than in these two taxa. Most other early eusauropods that have preserved this region preserved lack well developed proatlantal facets on the exoccipitals (e.g., *Spinophorosaurus*, *Nebulasaurus*, *Mamenchisaurus*, *Omeisaurus*). However, relatively well developed proatlantal facets are present in some non-neosauropod eusauropods (e.g., cf. *Cetiosaurus* OUMNH J13596, *Turiasaurus*, *Losillasaurus*) as well as in some diplodocoid and titanosaurian neosauropods [13]. In these taxa, however, the proatlantal facets are flat and smooth rather than elevated, convex, and rugose as in *Bagualia*.

6. *Concave ventral margin of the distal portion of the cultriform process*. The base of the cultriform process (or parasphenoid rostrum) of *Bagualia* is directed anterodorsally as in eusauropods, but this process is broken at its midpoint so that the anterior half is artificially directed anteroventrally. The anterior half is nonetheless well preserved and its ventral margin of is first straight but then becomes concave in lateral view (figures 2*e*, S6*b*). This ventrally concave margin extends for approximately one third of the total length of the cultriform process (approximately 19.4 mm). The cultriform process of other sauropodomorphs lack a distinct concavity along its ventral margin (e.g., *Adeopapposaurus*, *Anchisaurus*, *Mamenchisaurus*, *Europasaurus*) and therefore we consider this an autapomorphy of *Bagualia*.

7. *Axis with a large rounded anterior process in the distal end of the neural spine*. The axis of *Bagualia* is well preserved in the holotype (figure S8). The neural spine is relatively low at

its posterior end and its dorsal margin descends anteriorly so that the anterior region is located at the level of the postzygapophyses. The neural spine of *Bagualia* exceeds the anterior margin of the neural arch pedicels and bears a large rounded process at its anterior end (see apns in figure S8). This feature is absent in other early eusauropods such as *Shunosaurus* but an anterior process is present in two eusauropods, *Jobaria* and *Europasaurus.* In *Jobaria* this process differs from that of *Bagualia* in that is a sharp pointed process rather than a large rounded process. In the case of *Europasaurus* the process is also narrow and pointed but it also differs from that of *Bagualia* in that is located much higher and directed anteriorly rather than anteroventrally. Both *Jobaria* and *Europasaurus*, however, are distantly related to *Bagualia* and their similarities are interpreted as convergently acquired.

8. *Accessory lamina below the PCDL in middle cervical vertebrae*. This lamina is present both in the holotype of *Bagualia* (MPEF-PV 3301-16) and a middle cervical vertebra referred to this taxon (MPEF-PV 11040-2). This accessory lamina is located below the PCDL and runs anteroventrally, parallel to the ACDL (see al in detail of figure S11*a*). A similar lamina is also present in the rebbachisaurid *Nigersaurus* (MNN GAD 512) and the macronarian *Europasaurus* (accessory ACDL; [S14]). These two taxa, however, are phylogenetically distant from *Bagualia* and their similarity is interpreted as convergently acquired.

9. *EPRL present in middle cervical vertebrae*. The epiprezygapophyzeal lamina runs from the PODL towards the SPRL in middle cervical vertebrae of *Bagualia* (figures S9–S11). The EPRL is low and runs horizontally along the lateral surface of the neural spine and reaches the SPRL at the level of the anteroventral corner of the neural spine. Thus, the EPRL of *Bagualia* completely divides the spinodiapophyseal fossa. A similar EPRL has been reported for many neosauropods [15], as it has traditionally been recognized as a synapomorphic character of rebbachisaurids and certain macronarian taxa (e.g., *Camarasaurus*, *Euhelopus*, *Galvesaurus*). However, the presence of an EPRL outside Neosauropoda is very rare, and so far this lamina has only been described for the Early Cretaceous turiasaurian *Moabosaurus* ([S16]: fig. 13G, 14 B, 16

B) and some mamenchisaurids [13,15]. All the above-mentioned taxa are distantly related to *Bagualia* we consider this feature as independently acquired in the new species.

Skull. The rostrum of *Bagualia alba* is high and short as evidenced by the lateral surface of the premaxilla and maxilla. Based on the preserved elements the maxilla had a large participation on the margin of the external nares (figures 2*a*, S4), contributing to more than one third of its border. This feature is unique of eusauropods and contrasts with the short participation of the maxilla in the external nares in non-sauropod sauropodomorphs. The preserved margins of the antorbital fossa on the maxilla (figure S4) and on the lacrimal (figure 2*a*) lack a well-developed antorbital fossa, another featured exclusive of eusauropods. The anteroventral (premaxilla and maxilla) and posterodorsal (nasal) margins of the external nares have been preserved, the latter of which indicates the presence of a posteriorly retracted opening. The lacrimal has an extremely short anterior process as in many eusauropods [S17]. The prefrontal of *Bagualia* is long and narrow and extends posterodorsally approaching the frontoparietal suture, a feature that appears in eusauropods more derived than *Shunosaurus*. Furthermore, the prefrontal lacks the anterior process commonly present in non-sauropod sauropodomorphs. The postorbital descending process is long (figure 2) and transversely narrow, contrasting with the lateromedially broad descending process of neosauropods. The dorsal margin of the postorbital is lower than the dorsal margin of the parietal so that the supratemporal fenestra is exposed in lateral view, synapomorphic feature of eusauropods. As noted above the wide frontal participates briefly in the orbital margin and fails to enter the supratemporal fenestra (figure 2*b,* S5), derived features exclusive of Eusauropoda. The parietal exposure on the occipital surface is short, less than the height of the foramen magnum as in non-neosauropods. The quadrate of *Bagualia* lacks a quadrate fossa on its lateral surface (figure 2*j*), a plesiomorphic feature that distinguish the new taxon from all other eusauropods except for *Spinophorosaurus*. The braincase is very well preserved and shows many features that are phylogenetically relevant. The basal tubera are rounded and distally separated (figure 2*d*). They are placed only slightly ventral to the occipital condyle but dorsal to the basipterygoid processes (figure 2*d*–*e*) and are narrower than the

occipital condyle (figure 2*d*), a combination of features only found in early eusauropods (e.g., *Nebulasaurus* and *Spinophorosaurus*). In lateral view, the distal end of the basipterygoid processes are located close to the level of the basal tubera, as in eusauropods, rather than being located well anteriorly respect to the tubera (as in non-sauropod sauropodomorphs). The lateral surface of the basipterygoid processes bear groove and a crest located distal to the preotic pendant (see figure 2*e,* and c in S6*b*), which resembles the condition of neosauropods (e.g., *Camarasaurus*, *Diplodocus*) and likely indicates the course of the cerebral branch of the internal carotid artery. The preotic pendant (pp in figure 2*e* and S6*b*) is formed by the prootic dorsally and the basisphenoid ventrally and covers the entrance of the internal carotid artery, a condition also present in other eusauropods (e.g., *Spinophorosaurus*, *Camarasaurus, Diplodocus*) but absent in non-sauropods (e.g., *Adeopapposaurus*). Cranial pneumaticity is limited and the braincase lacks a basisphenoidal, subsellar or lateral tympanic recess (as in other eusauropods). The anterodorsal orientation of the base of the cultriform process is also a derived feature only present in eusauropods (figures 2*e,* S6*b*). The distal end of the paroccipital process is not expanded but it is located close to the level of the occipital condyle (figures 2*d,* S6*a*), which contrasts with the condition of non-sauropods in which this process is well above the condyle. The high supraoccipital (twice as deep as the foramen magnum; figures 2*d,* S6*a*) is also a derived feature only present in eusauropods.

Mandible. The lower jaw is represented in *Bagualia* by a left and right dentary (figure S7) and two right surangulars. The dentaries are well preserved in particular the left one. The mandibular symphysis is long and obliquely oriented at an angle of approximately 45 degrees (figure S7*c*). The symphyseal regions dorsoventrally deep and expanded respect to the rest of the dentary, so that the anterior ramus is approximately 1.5 times the height of the dentary at mid-length. This condition is present in several eusauropods, and also found in some early sauropodomorphs (e.g., *Mussaurus*). The dentaries of *Bagualia* are broadly curved (figure 2*c*) so that the mandibular rami form a U-shaped rostrum in dorsal view, a derived feature that is unique of eusauropods and that distinguish their lower jaw from that of more basal sauropodomorphs

([S17]; [S18]). The anteroventral margin of the dentary is gently rounded, different to other eusauropods that have a ventrally expanded corner or “chin” (e.g., *Shunosaurus, Mamenchisaurus*). The dentary bears only 16 tooth positions, a tooth count that is common among eusauropods but that is smaller than in more basal sauropodomorphs. The tooth count of *Bagualia* is also smaller than in the basal most eusauropod *Shunosaurus* and the eusauropod outgroup *Tazoudasaurus*. The lateral wall of the alveoli is markedly elevated respect to the medial martin, forming a well-developed lateral plate (a synapomorphic character of Eusauropoda [S19]). The alveoli are bordered lingually by fused interdental plates (figure S7*c*) which have nutrient foramina below to tooth row.

Dentition. The teeth of *Bagualia* are spatulate, with their crown broader than the root, a feature common in basal eusauropods, including basal macronarians ([S20]). The teeth are procumbent as in most sauropods with broad crowns [S21]. The crowns of all teeth have a convex labial surface and a concave lingual surface, which gives a D-shape in cross section (figure S3*c*). The apex of the crowns is slightly curved lingually. The mesial and distal margins are asymmetrical, being the mesial margin more convex than the distal margin which has a slightly concavity close the apex (figure 2*g*). The simultaneous presence of these features is only present in sauropods with spatulate crowns [S22], as non-sauropod sauropodomorphs only have a subset of these features. The lingual surface has apicobasal oriented grooves (figure 2*f–g*), as in many sauropodomorphs. The labial surface also bears apicobasal grooves near the mesial and distal margins of the crown (figure S3*c*), a character that has been considered as synapomorphic of eusauropods and their closest outgroups ([S17]; [S22]). The SI (i.e., slenderness index *sensu* [S18]) of the premaxillary, maxillary, and dentary teeth range between 1.1 and 1.6, with an average of 1.38. This range of values is congruent with those of sauropods with broad crowns (e.g., *Tazoudasaurus*, *Turiasaurus*, *Jobaria*) but the SI values are smaller than those of the teeth of *Patagosaurus*. The enamel is heavily wrinkled, a character traditionally considered as synapomorphic of Eusauropoda ([S18]; [S23]), but have a different pattern of wrinkling than the teeth of *Patagosaurus*. Further details and differences on the enamel wrinkling pattern were

pointed out by Holwerda et al [S24] in an analysis of the sauropod tooth morphotypes from the Cañadón Asfalto Formation, in which a tooth of *Bagualia* (MPEF-PV 3341) was recognized as morphotype III. Unworn teeth of *Bagualia* have well developed denticles on both the mesial and the distal margins of the crowns (figure 2*h*), a plesiomorphic feature commonly found in non-neosauropod sauropodomorphs [S17]. There are more denticles in the mesial margin than in the distal margin and they extend along the apical half of the crown. Towards the root, the enamel ends abruptly forming a step at the base of the crown, with a small enamel bulge at the mesial and distal regions (figure 2*g*). This condition contrasts with that of some sauropods in which the enamel becomes gradually thinner to disappear at the crown-root limit (e.g., *Amygdalodon*, *Patagosaurus*). The enamel layer is over 700 μm thick (figures 1, 2), a similar value to other eusauropods (e.g., *Patagosaurus*, *Camarasaurus*, *Diplodocus*), which represents an increase in enamel thickness compared to earlier sauropodomorphs (e.g., 153–156 μm thick in *Mussaurus*). CT scanning revealed up to three replacement teeth per position in the premaxilla (figure S3*c*), suggesting high dental replacement rates. In worn teeth the wear facets are V-shaped, which suggest an interlocking upper and lower jaw occlusion common in eusauropods but absent in non-sauropod sauropodomorphs [S25].

Vertebrae. The holotype of *Bagualia* includes the first seven articulated cervical vertebrae whereas the dorsal, sacral and caudal regions are represented by several disarticulated vertebrae found at the same site (see referred specimens below). All cervical vertebrae are opisthocoelous (a synapomorphy of the sauropod clade formed by *Amygdalodon* and more derived taxa; [S22]; figures S9, S11), differing from the amphicoelous/amphiplatyan condition of non-sauropod sauropodomorphs. The cervical vertebrae have elongated centra, with an elongation index of postaxial elements that ranges between 3 and 4.6 in the preserved elements of the holotype (figures S9–S11). These values indicate the presence of rather elongated middle cervical centra in *Bagualia* in comparison with other early eusauropods (e.g., *Patagosaurus*, *Shunosaurus*, *Spinophorosaurus*), but approaching the values present in certain Chinese taxa (e.g. *Omeisaurus*) and many neosauropods. Therefore, compared to *Patagosaurus* the vertebrae

of *Bagualia* are proportionally longer, indicating a different neck elongation in the two eusauropods from the Cañadón Asfalto Formation. The cervical centra bear a well-developed ventral keel (a plesiomorphic character among eusauropods; see vk in figures S9, S11) and marked pleurocoels (a derived character of eusauropods; see pl in figures S9–S11). The pleurocoels are anteriorly deep and become shallow posteriorly, as is common in other non-neosauropod eusauropods (e.g., *Patagosaurus*, *Spinophorosaurus*) and they are undivided, also a feature present in early sauropods (e.g., *Tazoudasaurus*, *Shunosaurus*, *Cetiosaurus*). In contrast, in dorsal and sacral vertebrae lack pleurocoels in their centra, as it also occurs in some early eusauropods. The diapophyses of cervical vertebrae have a triangular process on the posterior margin, a feature convergently appearing in certain eusauropods (e.g., *Shunosaurus*, *Jobaria*) and neosauropods (e.g., *Amargasaurus*). The entire presacral series of *Bagualia* have well-developed laminae, including the axis (figure S9). Among these laminae, the presence of PCPL in the dorsal vertebrae and of a well-developed PRDL in anterior caudal vertebrae is a derived feature present in eusauropods and more derived taxa. In middle and posterior dorsal vertebrae there is a divided SPOL, another derived feature only present in certain Jurassic eusauropods (*Spinophorosaurus*, *Patagosaurus* and *Omeisaurus*) and several neosauropods. The dorsal neural spines are wider lateromedially than anteroposteriorly, a feature that has been considered as synapomorphy of Eusauropoda ([S17]; [S26]).

List of Materials

The holotype of *Bagualia alba* MPEF PV 3301 consists of a posterior half of a skull found in articulation with seven cervical vertebrae. The skull elements were found in partial articulation and some of them were disarticulated during mechanical preparation. Other cranial materials found in the bonebed include repeated elements (e.g., maxillae, dentaries, surangulars) and multiple isolated teeth that show no differences and support the interpretation of this assemblage as a monospecific accumulation of elements. A complete list of craniomandibular elements is detailed below:

MPEF-PV	3305	Left premaxilla (Fig. S3)
MPEF-PV	3304	Left maxilla
MPEF-PV	3341a	Left maxilla (Fig. S4)
MPEF-PV	3204	Right maxilla
MPEF-PV	3202-3	Right dentary (Fig. S7)
MPEF-PV	3202-1	Left dentary
MPEF-PV	3202-2	Right surangular
MPEF-PV	3339	Right surangular
MPEF-PV	3340	Right nasal

Several dentigerous elements preserved teeth in the natural position and additionally multiple isolated teeth were found in the quarry, which are listed below:

MPEF-PV 3146

MPEF-PV 3174

MPEF-PV 3175

MPEF-PV 3176

MPEF-PV 3203

MPEF-PV 3205

MPEF-PV 3207

MPEF-PV 3208

MPEF-PV 3209

MPEF-PV11030

MPEF-PV11031

MPEF-PV11032

MPEF-PV 11033

MPEF-PV 11034

MPEF-PV 11035

MPEF-PV 11036

MPEF-PV 11038

MPEF-PV 11039

MPEF-PV 11041

MPEF-PV 11042

MPEF-PV 11045

The postcranial materials include the cervical vertebrae of the holotype (Fig. S8–S11) and also include other repeated elements (e.g., scapula, coracoids, humeri, fibulae, ilia, pubes, ischia, femora, ulnae) that show no differences and support the interpretation of this assemblage as a monospecific accumulation of elements. A complete list of postcranial elements is detailed here:

MPEF-PV 3408 Cervical vertebra

MPEF-PV 3327 Cervical vertebra

MPEF-PV 3348 Cervical vertebra

MPEF-PV 3349 Cervical vertebra

MPEF-PV 11040 Cervical vertebrae

MPEF-PV 11023 Dorsal vertebra

MPEF-PV 11027 Dorsal vertebra

MPEF-PV 11000 Dorsal vertebra

MPEF-PV 3300 Caudal vertebra

MPEF-PV 3319 Caudal vertebra

MPEF-PV 3322 Caudal vertebra

MPEF-PV 3324 Caudal vertebra

MPEF-PV 3331 Caudal vertebra

MPEF-PV 3346 Caudal vertebra

MPEF-PV 11044 Caudal vertebrae

MPEF-PV 3356 Haemal arch

MPEF-PV 11025 Haemal arch

MPEF-PV 3351 Haemal arch

MPEF-PV 3352 Haemal arch

MPEF-PV 3353 Haemal arch

MPEF-PV 3354 Haemal arch

MPEF-PV 3355 Haemal arch

MPEF-PV 3357 Haemal arch

MPEF-PV 3358 Haemal arch

MPEF-PV 3359 Haemal arch

MPEF-PV 3390 Haemal arch

MPEF-PV 11009 Haemal arch

MPEF-PV 11010 Haemal arch

MPEF-PV 11011 Two dorsal neural arches with a partial sacrum with both ilia and the first ten caudal vertebrae

MPEF-PV 3382 Scapula

MPEF-PV 3383 Scapula

MPEF-PV 3384 Scapula

MPEF-PV 3385 Scapula

MPEF-PV 3386-a Scapula

MPEF-PV 11015 Coracoid

MPEF-PV 3387 Coracoid

MPEF-PV 3386-b Coracoid

MPEF-PV 3385 Coracoid

MPEF-PV 3311 Humerus

MPEF-PV 3338 Humerus

MPEF-PV 3380 Humerus

MPEF-PV 3381 Humerus

MPEF-PV 11020 Humerus

MPEF-PV 3312 Ulna

MPEF-PV 3379 Ulna

MPEF-PV 3313 Radius

MPEF-PV 3332 Metacarpal

MPEF-PV 3333 Metacarpal

MPEF-PV 3334 Metacarpal

MPEF-PV 3369 Ilium

MPEF-PV 3377 Pubis

MPEF-PV 11019 Pubis

MPEF-PV 3337 Ischium

MPEF-PV 11016 Ischium

MPEF-PV 3371 Femur

MPEF-PV 11024 Femur

MPEF-PV 3303 Femur

MPEF-PV 11021 Femur

MPEF-PV 11022 Femur

MPEF-PV 3374 Tibia

MPEF-PV 3376 Fibula

MPEF-PV 3306 a-b Fibula

MPEF-PV 3307 Astragalus

MPEF-PV 3308 Astragalus

MPEF-PV 11018 Calcaneum

MPEF-PV 3335 Phalanx

MPEF-PV 11028 Phalanx

MPEF-PV 11029 Phalanx

MPEF-PV 11049 Phalanx

MPEF-PV 3310 Ungual phalanx

MPEF-PV 3410 Ungual phalanx

Phylogenetic Analysis

Phylogenetic dataset. The phylogenetic analysis was based on a compilation of previously published data matrices focused on both eusauropods [S17, S26–S29] and those focused on basal sauropodomorphs [S30–S33].

Taxon sampling also focused on integrating species of Eusauropoda along with non-eusauropod sauropodomorphs recorded in the Late Triassic and Early Jurassic. A total of 27 non-eusauropod and 89 eusauropods were included in the data matrix. In addition to the taxa included in the above-mentioned matrices, we scored *Bagualia alba* and four recently published sauropodomorphs. Two of these were scored based only on literature (*Tonganosaurus hei* [S34], *Yizhousaurus sunae* [S35]) and the other two were also scored with first hand revision of the specimens (*Sanpasaurus yaoi* [S36] and NHMUK PV R36834 [S37]).

Character compilation of these sources resulted in a total of 499 characters including cranial and postcranial features, including one new character (character 475). We modified three characters (104, 371, and 15) from a previous dataset [S29]. See below for a complete list of characters (data matrix available in Dataset S1).

Phylogenetic analysis. Our results and discussion are based on an equally weighted parsimony analysis although we additional analyses under other optimality criteria (see below Alternative phylogenetic analyses). The parsimony analysis was conducted in TNT 1.5 [S38] through a heuristic search with 1,000 replicates of Wagner trees (with random addition sequence) followed by TBR branch swapping (holding 10 trees per replicate). A subsequent search was conducted performing a round of TBR branch swapping on the most parsimonious trees (MPTs). Bremer support values were calculated using the script *bremsup.run* and jackknife resampling analysis was performed using 100 pseudoreplicates and calculating absolute and GC frequencies. The low support values retrieved prompted us to conduct further support analyses with the main objective of evaluating how well supported was the inclusion of *Bagualia* in Eusauropoda. Firstly, we applied the *pcrjak* procedure proposed by Pol and Goloboff [S39] to test if phylogenetically unstable and/or fragmentary specimens were masking underlying support for basal nodes of

Eusauropoda. Secondly, we conducted parsimony analyses under constraints to test how suboptimal were alternative phylogenetic placements of *Bagualia*. Thirdly, we conducted a Templeton test to evaluate for six alternative placements of *Bagualia* (three in more basal position than in the optimal position and three in more derived position than in the MPTs) using the implementation of this test in a script for TNT [S40]. For each of the 6,000 MPTs obtained in the original parsimony search we placed *Bagualia* in the six alternative placements and we conducted a Templeton test to compare the original with the altered topology (totalling 36,000 independent Templeton tests).

Tree Search Results. The equally weighted parsimony analysis recovered 410 MPTs of 1914 steps (CI=0.309, RI=0.723) found in 46 of the 1,000 replicates. The second round of TBR branch swapping resulted in 6,000 MPTs. The strict consensus (Fig. S12) has a large polytomy in basal nodes of Sauropodomorpha and a smaller polytomy in the basal nodes of Sauropoda. *Bagualia* is unequivocally placed within Eusauropoda. Applying the IterPCR implementation of TNT [S38] identifies 8 unstable taxa as causing this large polytomies. Ignoring their position in the MPTs results in a much more resolved reduced strict consensus (figure S13).

Support analysis. Bremer and Jackknife support analyses show overall low support values in the tree, including those of several nodes close to the base of Eusauropoda. Bremer support analysis, for instance, revealed minimal values for most basal nodes of Eusauropoda (figure S14). The low values of Bremer support, however, do not necessarily indicate that the inclusion of *Bagualia* in this clade is not well supported. The instability of other taxa can produce low support values, a phenomenon shown by Wilkinson et al. [S41] and frequently found when fragmentary specimens are included phylogenetic analyses. Similarly, the results of parsimony jackknife analysis (figure S15) reveals low support values for many basal nodes of Eusauropoda. The grouping of *Bagualia* with *Nebulasaurus* and *Spinophorosaurus*, however, is one of the few nodes of basal eusauropods that is retrieved in the majority rule tree (i.e., > 50%) of the jackknife analysis (figure S15).

These low support values are likely heavily influenced by the highly fragmentary nature of many basal sauropods and eusauropods, as the abundance of missing data can lead to phylogenetically instability and this may obscure underlying support for certain groups [S41]. In order to overcome this problem, we applied the *pcrjak* procedure proposed by Pol and Goloboff [S39] that detects unstable taxa and produces a reduced jackknife analysis showing the groupings of stable taxa that are well supported by the data. The results of the *pcrjak* procedure (figure S16) show overall good support for the inclusion of *Bagualia* in Eusauropoda, as the latter clade is retrieved in 76% of the replicates when unstable taxa are ignored. Furthermore, the grouping of *Bagualia* with *Spinophorosaurus* and *Patagosaurus* to the exclusion of other eusauropods is present in 75% of the jackknife replicates when unstable taxa are ignored from the results (figure S16).

To further test the robustness of the inclusion of *Bagualia* within Eusauropoda we also tested various alternative placements of the new taxon. The results of these exploratory analyses show that *Bagualia* is well supported as an early eusauropod, although there is much less support for defining its precise placement within the basal nodes of Eusauropoda.

Constrained parsimony searches forcing *Bagualia* in different positions show that trees that place this taxon outside Eusauropoda are markedly suboptimal (e.g., placing *Bagualia* basal to *Shunosaurus* implies at least 12 extra steps). Similarly, forcing *Bagualia* to take positions close to Neosauropoda implies at least 8 extra steps (e.g., allied with turiasaurians or as the sister group of *Jobaria* and Neosauropoda). Conversely, trees depicting *Bagualia* only slightly more basal or more derived than in the MPTs show various degrees of suboptimality. For instance, placing *Bagualia* basal to *Barapasaurus* implies 7 extra steps and placing it as the sister group to turiasaurians and more derived eusauropods implies 5 extra steps.

Templeton tests show that trees placing *Bagualia* outside Eusauropoda or in the most basal nodes of this clade (e.g., basal to *Barapasaurus*) are significantly worse explanations of the analysed data matrix (p-values in comparisons of the 6,000 MPTs range between 0.0029 and 0.0112 for the former position and range between 0.0102 and 0.0425 for the latter position). Similarly, topologies that place *Bagualia* close to Neosauropoda are also rejected as significantly

worse explanation of the analysed data (e.g., p-values for comparisons when *Bagualia* is the sister group of Jobaria and Neosauropoda or clustered with Turiasauria range between 0.0039 and 0.0078). On the other hand, many trees that place *Bagualia* in a slightly more basal or more derived position than in the MPTs cannot be rejected as significantly worse explanations of the data. Non-significant differences are commonly found in topologies in which *Bagualia* is placed as more derived than *Barapasaurus* (p-values up to 0.1055) and more basal than Turiasauria (p-values up to 0.0625). These results indicate character data in our matrix provide good support for considering *Bagualia* as an early eusauropod.

Alternative phylogenetic analyses. In addition to the equally weighted parsimony analysis described above we performed alternative phylogenetic analyses using our data matrix, including variants of the parsimony criterion and a Bayesian analysis. The parsimony variants were also run in TNT and included analyses under implied weights [S42] and extended implied weights [S43]. For each of these variants we used three different concavity (K) values (5, 10, and 15). The six analyses differ in some details of the obtained topologies, but almost all of them place *Bagualia* in a small clade of early eusauropods along with *Nebulasaurus*, *Spinophorosaurus*, and *Patagosaurus* (as in the equally weighted analysis). The only exception to this result is the use of extended implied weighting and the lowest concavity value (K=5) that place *Bagualia* basal to these taxa but more derived than *Barapasaurus* and *Shunosaurus*. Irrespective of these topological differences, all analyse under implied weights agree in the inclusion of *Bagualia* within Eusauropoda. In addition to the implied weight analyses we run an equally weighted parsimony analysis with all characters set as unordered, which also resulted in topologies that place *Bagualia* in a small clade of early eusauropods along with *Nebulasaurus*, *Spinophorosaurus*, and *Patagosaurus* (as in the original analysis). Finally, we run a Bayesian analysis for this dataset using MrBayes under the Mkv model [S44] which also depicts *Bagualia* as an early eusauropod. The Bayesian analysis places *Bagualia* in the same small clade along with *Nebulasaurus*, *Spinophorosaurus*, and *Patagosaurus* (a clade with a 0.85 posterior probability). These results

that the phylogenetic position in which we based our results and discussion (using equally weighted parsimony) is not sensitive to the choice of optimality criterion.

Synapomorphy list. The following list of unambiguous synapomorphies were obtained from the pool of 6,000 most parsimonious trees resultant from the equally weighted parsimony analysis. Node numbers refer to those present in Figure S12

Node 107 :

All trees:

Char. 57: 0 --> 1

Char. 384: 0 --> 1

Char. 478: 0 --> 1

Char. 479: 0 --> 1

Char. 480: 1 --> 0

Char. 491: 1 --> 0

Some trees:

Char. 379: 1 --> 0

Node 108 :

All trees:

Char. 112: 1 --> 0

Char. 496: 1 --> 2

Node 109 :

All trees:

No synapomorphies

Node 110 :

Some trees:

Char. 13: 0 --> 1

Char. 100: 0 --> 1

Char. 103: 01 --> 2

Char. 233: 1 --> 0

Char. 298: 0 --> 1

Char. 299: 0 --> 1

Char. 300: 0 --> 1

Char. 335: 0 --> 1

Char. 382: 0 --> 1

Char. 390: 0 --> 1

Char. 399: 0 --> 1

Char. 400: 0 --> 1

Char. 408: 0 --> 1

Char. 409: 0 --> 1

Char. 430: 1 --> 2

Char. 460: 1 --> 2

Node 111 :

All trees:

Char. 448: 1 --> 2

Node 112 :

All trees:

Char. 153: 0 --> 1

Char. 410: 0 --> 1

Node 113 :

Some trees:

Char. 99: 0 --> 1

Char. 160: 0 --> 1

Char. 383: 0 --> 1

Char. 424: 0 --> 1

Node 114 :

All trees:

Char. 117: 1 --> 0

Some trees:

Char. 181: 0 --> 1

Char. 229: 0 --> 1

Char. 261: 0 --> 1

Char. 314: 0 --> 1

Node 115 :

All trees:

Char. 126: 0 --> 1

Some trees:

Char. 113: 0 --> 1

Char. 154: 0 --> 1

Char. 180: 1 --> 2

Char. 182: 0 --> 1

Char. 375: 1 --> 0

Char. 448: 1 --> 2

Node 116 :

All trees:

Char. 153: 0 --> 1

Char. 255: 1 --> 0

Char. 388: 0 --> 1

Char. 404: 0 --> 1

Some trees:

Char. 215: 1 --> 2

Char. 307: 1 --> 0

Char. 353: 0 --> 1

Node 117 :

All trees:

Char. 127: 1 --> 0

Char. 385: 0 --> 1

Node 118 :

All trees:

Char. 42: 0 --> 1

Char. 369: 0 --> 1

Char. 421: 2 --> 1

Node 119 :

All trees:

Char. 114: 0 --> 2

Char. 123: 0 --> 1

Char. 134: 0 --> 1

Char. 138: 0 --> 3

Char. 141: 0 --> 1

Char. 173: 0 --> 2

Some trees:

Char. 105: 0 --> 1

Char. 108: 2 --> 4

Char. 111: 0 --> 1

Char. 113: 1 --> 2

Char. 119: 0 --> 12

Char. 124: 1 --> 0

Char. 125: 0 --> 1

Char. 144: 0 --> 1

Char. 186: 1 --> 0

Char. 236: 0 --> 1

Char. 307: 1 --> 0

Char. 385: 0 --> 1

Char. 419: 12 --> 0

Node 120 :

All trees:

Char. 141: 0 --> 1

Char. 173: 0 --> 1

Char. 192: 0 --> 2

Node 121 :

Some trees:

Char. 112: 0 --> 1

Char. 113: 1 --> 2

Char. 134: 0 --> 1

Char. 147: 0 --> 1

Char. 295: 0 --> 1

Char. 447: 0 --> 1

Node 122 :

All trees:

Char. 114: 0 --> 1

Char. 148: 0 --> 1

Char. 206: 0 --> 1

Char. 308: 0 --> 1

Char. 316: 0 --> 1

Char. 318: 0 --> 1

Some trees:

Char. 309: 0 --> 1

Node 123 :

All trees:

Char. 141: 0 --> 1

Char. 160: 1 --> 0

Char. 185: 0 --> 1

Char. 235: 0 --> 1

Node 124 :

All trees:

Char. 22: 0 --> 1

Char. 105: 0 --> 2

Char. 119: 0 --> 1

Some trees:

Char. 353: 1 --> 0

Char. 373: 01 --> 0

Node 125 :

All trees:

Char. 198: 0 --> 1

Char. 392: 0 --> 1

Node 126 :

All trees:

Char. 115: 1 --> 2

Char. 135: 1 --> 0

Char. 142: 0 --> 1

Char. 237: 0 --> 1

Char. 287: 0 --> 1

Char. 292: 0 --> 1

Char. 316: 1 --> 0

Some trees:

Char. 374: 1 --> 0

Node 127 :

All trees:

Char. 111: 0 --> 1

Char. 119: 1 --> 2

Char. 179: 0 --> 1

Char. 192: 0 --> 1

Char. 301: 0 --> 1

Node 128 :

All trees:

Char. 73: 0 --> 1

Char. 210: 0 --> 1

Char. 259: 0 --> 1

Char. 281: 0 --> 1

Char. 283: 0 --> 1

Char. 415: 1 --> 0

Some trees:

Char. 358: 0 --> 1

Node 129 :

All trees:

Char. 357: 0 --> 1

Some trees:

Char. 251: 1 --> 2

Char. 368: 0 --> 1

Node 130 :

All trees:

Char. 212: 2 --> 0

Node 131 :

All trees:

Char. 257: 0 --> 1

Node 132 :

All trees:

Char. 236: 0 --> 1

Char. 237: 0 --> 1

Char. 258: 0 --> 1

Node 133 :

All trees:

Char. 120: 0 --> 1

Char. 122: 0 --> 1

Char. 244: 1 --> 0

Char. 375: 0 --> 2

Char. 413: 1 --> 0

Some trees:

Char. 358: 1 --> 0

Node 134 :

Some trees:

Char. 117: 0 --> 1

Char. 140: 1 --> 0

Char. 148: 1 --> 2

Char. 150: 0 --> 1

Char. 151: 0 --> 2

Char. 306: 0 --> 1

Char. 310: 0 --> 1

Char. 473: 0 --> 1

Node 135 :

All trees:

Char. 147: 2 --> 1

Char. 156: 2 --> 0

Node 136 :

All trees:

Char. 29: 0 --> 1

Char. 60: 0 --> 1

Char. 69: 1 --> 0

Char. 76: 0 --> 1

Node 137 :

All trees:

Char. 0: 1 --> 0

Char. 1: 1 --> 0

Char. 11: 1 --> 2

Char. 82: 0 --> 1

Char. 415: 0 --> 1

Node 138 :

All trees:

Char. 125: 1 --> 0

Char. 354: 0 --> 1

Some trees:

Char. 188: 1 --> 2

Char. 241: 0 --> 1

Char. 242: 0 --> 1

Char. 266: 0 --> 1

Char. 362: 0 --> 1

Char. 392: 0 --> 1

Node 139 :

All trees:

Char. 139: 1 --> 0

Char. 194: 0 --> 1

Char. 212: 1 --> 2

Char. 243: 1 --> 0

Char. 245: 0 --> 1

Char. 255: 1 --> 2

Char. 263: 0 --> 1

Char. 360: 0 --> 1

Node 140 :

All trees:

Char. 135: 0 --> 1

Char. 217: 0 --> 1

Char. 240: 1 --> 0

Char. 364: 1 --> 0

Some trees:

Char. 136: 0 --> 1

Char. 149: 2 --> 1

Node 141 :

All trees:

Char. 202: 1 --> 0

Char. 207: 0 --> 1

Node 142 :

All trees:

Char. 0: 1 --> 0

Char. 1: 1 --> 0

Char. 6: 0 --> 1

Char. 8: 0 --> 1

Char. 18: 0 --> 2

Char. 19: 0 --> 1

Char. 21: 0 --> 1

Char. 54: 0 --> 1

Char. 55: 0 --> 1

Char. 57: 1 --> 2

Char. 77: 0 --> 1

Char. 93: 1 --> 2

Char. 94: 1 --> 3

Char. 96: 0 --> 1

Char. 99: 1 --> 0

Char. 101: 0 --> 1

Char. 102: 1 --> 3

Char. 107: 0 --> 3

Char. 111: 0 --> 1

Char. 144: 1 --> 2

Char. 162: 1 --> 0

Char. 183: 0 --> 1

Char. 198: 0 --> 1

Char. 204: 0 --> 1

Char. 214: 0 --> 1

Char. 218: 0 --> 1

Char. 219: 0 --> 1

Char. 368: 0 --> 1

Char. 377: 0 --> 1

Char. 382: 1 --> 0

Node 143 :

Some trees:

Char. 165: 0 --> 1

Char. 191: 0 --> 1

Node 144 :

Some trees:

Char. 151: 0 --> 1

Char. 192: 0 --> 4

Char. 288: 0 --> 1

Node 145 :

All trees:

Char. 237: 0 --> 1

Some trees:

Char. 151: 1 --> 2

Char. 172: 0 --> 1

Node 146 :

All trees:

Char. 255: 1 --> 0

Char. 289: 0 --> 1

Char. 297: 0 --> 1

Node 147 :

All trees:

Char. 238: 0 --> 1

Node 148 :

All trees:

Char. 157: 0 --> 1

Char. 196: 0 --> 1

Char. 290: 0 --> 1

Char. 302: 0 --> 1

Node 149 :

All trees:

Char. 3: 0 --> 1

Char. 25: 0 --> 1

Char. 33: 1 --> 0

Char. 42: 0 --> 1

Char. 49: 0 --> 1

Char. 83: 0 --> 1

Char. 84: 0 --> 1

Char. 102: 3 --> 2

Char. 370: 1 --> 0

Node 150 :

All trees:

Char. 7: 0 --> 1

Char. 11: 1 --> 2

Char. 52: 1 --> 0

Char. 81: 0 --> 1

Char. 131: 0 --> 1

Char. 157: 0 --> 1

Char. 192: 0 --> 2

Char. 197: 0 --> 1

Char. 215: 1 --> 2

Char. 285: 0 --> 1

Char. 294: 1 --> 0

Char. 295: 1 --> 0

Char. 296: 0 --> 1

Char. 326: 0 --> 1

Char. 416: 0 --> 1

Char. 445: 1 --> 0

Node 151 :

All trees:

Char. 34: 0 --> 1

Char. 46: 0 --> 1

Char. 112: 1 --> 0

Char. 114: 12 --> 3

Char. 134: 1 --> 0

Char. 138: 1 --> 0

Node 152 :

All trees:

Char. 170: 0 --> 1

Node 153 :

All trees:

Char. 125: 0 --> 1

Char. 128: 0 --> 1

Char. 193: 0 --> 1

Char. 194: 0 --> 1

Char. 195: 0 --> 1

Char. 203: 0 --> 1

Char. 207: 0 --> 2

Char. 208: 0 --> 1

Char. 212: 2 --> 3

Char. 375: 2 --> 1

Node 154 :

All trees:

Char. 24: 0 --> 1

Char. 26: 0 --> 1

Char. 27: 0 --> 1

Char. 108: 1 --> 3

Char. 119: 1 --> 2

Char. 133: 2 --> 3

Char. 135: 1 --> 0

Char. 153: 0 --> 1

Char. 200: 0 --> 1

Char. 201: 0 --> 1

Char. 205: 0 --> 1

Node 155 :

All trees:

Char. 471: 0 --> 1

Char. 484: 0 --> 1

Some trees:

Char. 8: 0 --> 1

Char. 485: 0 --> 1

Char. 490: 0 --> 1

Node 156 :

All trees:

Char. 487: 1 --> 0

Char. 489: 1 --> 0

Some trees:

Char. 30: 0 --> 1

Char. 94: 01 --> 1

Char. 125: 0 --> 1

Char. 431: 1 --> 0

Node 157 :

Some trees:

Char. 144: 1 --> 0

Char. 152: 0 --> 1

Char. 224: 1 --> 0

Char. 229: 1 --> 0

Char. 358: 1 --> 0

Char. 374: 0 --> 1

Char. 390: 1 --> 0

Node 158 :

All trees:

Char. 262: 1 --> 0

Node 159 :

All trees:

Char. 255: 1 --> 0

Node 160 :

All trees:

Char. 18: 1 --> 0

Char. 255: 0 --> 2

Char. 263: 0 --> 1

Char. 390: 0 --> 1

Char. 434: 0 --> 1

Character list.

(1) Posterolateral processes of premaxilla and lateral processes of maxilla, shape: without midline contact (0); with midline contact forming marked narial depression, subnarial foramen not visible laterally (1). ([S29]:ch. 1).

(2) Premaxillary anterior margin shape: without step (0); with marked step but short step (1); with marked and long step (2) (modified from [S29]:ch. 2).

(3) Premaxila, ascending process shape in lateral view: convex (0); concave, with a large dorsal projection (1); sub-rectilinear and directed posterodorsally (2). ([S45]:ch. 3)

(4) Premaxilla, external surface: without anteroventrally orientated vascular grooves originating from an opening in the maxillary contact (0); vascular grooves present (1). ([S45]:ch. 2)

(5) Maxillary border of external naris, length: short, making up much less than one-fourth narial perimeter (0); long, making up more than one third narial perimeter (1). ([S29]:ch. 3).

(6) Maxilla, foramen anterior to the preantorbital fenestra: absent (0); present (1). ([S46]:ch. 244).

(7) Preanteorbital fenestra: absent (0); present, being wide and laterally opened (1). (Modified from [S29]:ch.4).

(8) Subnarial foramen and exterior maxillary foramen, position: well distanced from one another (0); separated by narrow bony isthmus (1). ([S29]:ch. 5)

(9) Antorobital fenestra: much shorter than orbital maximum diameter, less than 85% of orbit (0); subequal to orbital maximum diameter, greater than 85% orbit (1). (Modified from [S29]:ch. 6 following to [S45]:ch. 13)

(10) Antorbital fenestra, shape of dorsal margin: straight or convex (0); concave (1). ([S45]:ch. 14).

(11) Antorbital fossa: present (0); absent (1). ([S29]:ch. 7)

(12) External nares position: terminal (0); retracted to level of orbit (1); retracted to a position between orbits (2). ([S29]:ch. 8). **Ordered**.

(13) External nares, maximum diameter: shorter (0); or longer than orbital maximum diameter (1). ([S29]:ch. 9)

(14) Orbital ventral margin, anteroposterior length: broad, with subcircular orbital margin (0); reduced, with acute orbital margin (1). ([S29]:ch. 10)

(15) Lacrimal, anterior process: poorly developed, being its anteroposterior length approximately less than 30% the dorsoventral height of the bone (0); well developed (1). (Modified from [S29]:ch. 11)

(16) Jugal contribution to the ventral border of the skull: present and long (0); absent or very reduced (1). ([S47]:ch. 16).

(17) Quadratojugal-Maxilla contact: absent or small (0); broad (1). ([S45]:ch. 10).

(18) Jugal-ectopterygoid contact: present (0); absent (1). ([S29]:ch. 12)

(19) Jugal, contribution to antorbital fenestra: absent (0); present, but very reduced (1); present and large, bordering approximately one-third its perimeter (2). (Modified from

[S29]:ch. 13).

(20) Quadratojugal, position of anterior terminus: posterior to middle of orbit (0); anterior margin of orbit or beyond (1). ([S45]:ch. 30).

(21) Quadratojugal, anterior process length: short, anterior process shorter than dorsal process (0); long, anterior process more than twice as long as dorsal process (1). ([S29]:ch. 32)

(22) Quadratojugal, angle between anterior and dorsal processes: less than or equal to 90°, so that the quadrate shaft is directed dorsally (0); greater than 90°, approaching 130°, so that the quadrate shaft slants posterodorsally (1). [S45]:ch. 31).

(23) Ventral edge of anterior surface of the quadratojugal: straigth, not expanded ventrally (0); Slightly expanded ventrally, forming a small bulge, which height is less than twice the ramus height (1); well expanded ventrally, forming a notorious bulge, which height is twice or more the minimum height of the ramus (2). (Modified from [S48]:ch. 26)

(24) Squamosal contribution to the supratemporal fenestra: present, the squamosal is well visible in dorsal view (0); reduced or absent (1). ([S49]:ch. 37).

(25) Squamosal-quadratojugal contact: present (0); absent (1). ([S29]:ch. 31)

(26) Squamosal, posteroventral margin: smooth (0); "with prominent, ventrally directed ""prong"" (1). ([S45]:ch. 37).

(27) Prefrontal posterior process size: small, not projecting far posterior of frontal-nasal suture (0); elongate, approaching parietal (1). ([S29]:ch. 14)

(28) Prefrontal, posterior process shape: flat (0); hooked (1). ([S29]:ch. 15)

(29) Prefrontal, anterior process: absent (0); present (1). ([S49]:ch. 30)

(30) Prefrontal-Frontal contact width: large, equal or longer that the anteroposterior length of the prefrontal (0); narrow, less than half the anteroposterior length of the prefrontal (1). ([S46]:ch. 239).

(31) Postorbital, ventral process shape: transversely narrow (0); broader transversely than anteroposteriorly (1). ([S29]:ch. 16).

(32) Postorbital, posterior process: present (0); absent (1). ([S29]:ch. 17).

(33) Postorbital, posterior margin articulating with the squamosal: with tapering posterior process (0); with a deep posterior process (1). ([S46]:ch. 245).

(34) Frontal contribution to supratemporal fenestra: present (0); absent (1). (Modified from [S29]:ch. 18)

(35) Frontals, midline contact (symphysis): sutured (0); or fused in adult individuals (1). ([S29]:ch. 19)

(36) Frontal, anteroposterior length: approximately twice (0); or less than minimum transverse breadth (1). ([S29]:ch. 20)

(37) Frontal-nasal suture, shape: flat or slightly bowed anteriorly (0); V-shaped, pointing posteriorly (1). ([S45]:ch. 21)

(38) Frontals, dorsal surface: without paired grooves facing anterodorsally (0); grooves present, extend on to nasal (1). ([S45]:ch. 22)

(39) Frontal, contribution to dorsal margin of orbit: contribution to dorsal margin of orbit: less than 1.5 times the contribution of prefrontal (0); at least 1.5 times the contribution of prefrontal (1). ([S45]:ch. 23)

(40) Parietal occipital process, dorsoventral height: short, less than the diameter of the foramen magnum (0); deep, nearly twice the diameter of the foramen magnum (1). ([S29]:ch.21)

(41) Parietal, contribution to post-temporal fenestra: present (0); absent (1). ([S29]:ch. 22)

(42) Parietal, distance separating supratemporal fenestrae: less than the lateromedial axis of supratemporal fenestra, 0.8 or less (0); almost the same than the lateromedial axis of supratemporal fenestra 0.8-1.2 (1); much larger than the lateromedial axis of supratemporal fenestra more than 1.2 (2). (Modified from [S29]: ch. 24).

(43) Postparietal foramen: absent (0); present (1). ([S29]:ch. 23)

(44) Paroccipital process distal terminus:: straight, slightly expanded surface (0); rounded, tongue-like process (1). ([S45]:ch. 42)

(45) Supratemporal fenestra: present (0); absent (1). ([S29]:ch. 25)

(46) Supratemporal fenestra, long axis orientation: anteroposterior (0); transverse (1).

([S29]:ch.26)

(47) Supratemporal fenestra, maximum diameter: much longer than (0); or subequal to that of foramen magnum (1). ([S29]:ch. 27)

(48) Supratemporal region, anteroposterior length: temporal bar longer (0); or shorter anteroposteriorly than transversely (1). ([S29]:ch. 28)

(49) Supratemporal fenestra, lateral exposure: not visible laterally, obscured by temporal bar (0); visible laterally, temporal bar shifted ventrally (1). (Modified from [S29]:ch. 29)

(50) Supraoccipital, sagital nuchal crest: broad, weakly developed (0); narrow, sharp and distinct (1). ([S45]:ch. 45).

(51) Laterotemporal fenestra, anterior extension: posterior to orbit (0); ventral to orbit (1). ([S29]:ch. 30)

(52) Quadrate fossa: absent (0); present (1). ([S29]:ch. 33)

(53) Quadrate fossa, depth: shallow (0); deeply invaginated (1). ([S29]:ch. 34)

(54) Quadrate fossa, orientation: posterior (0); posterolateral (1). ([S29]:ch. 35)

(55) Quadrate, articular surface shape: quadrangular in ventral view, oriented transversely (0); roughly triangular in shape or thin, crescent-shaped surface with anteriorly directed medial process (1). (Modified sensu [S50]. from [S45]:ch. 32).

(56) Quadrate, articular surface shape: quadrangular in ventral view, oriented transversely or roughly triangular in shape (0); thin, crescent-shaped surface with anteriorly directed medial process (1). (Modified sensu [S50] from [S45]:ch. 32).

(57) Palatobasal contact, shape: pterygoid with small facet (0); dorsomedially orientated hook (1); or rocker-like surface for basipterygoid articulation (2). ([S29]:ch. 36)

(58) Pterygoid, transverse flange (i.e. ectopterygoid process) position: posterior of orbit (0); between orbit and antorbital fenestra (1); anterior to antorbital fenestra (2). ([S29]:ch.37). **Ordered**.

(59) Pterygoid, quadrate flange size: large, palatobasal and quadrate articulations well separated (0); small, palatobasal and quadrate articulations approach (1). ([S29]:ch. 38)

(60) Pterygoid, palatine ramus shape: straight, at level of dorsal margin of quadrate ramus (0); stepped, raised above level of quadrate ramus (1). ([S29]:ch.39)

(61) Pterygoid, sutural contact with ectopterygoid: broad, along the medial or lateral surface (0); narrow, restricted to the anterior tip of the ectopterygoid (1). (Zaher et al. 2011:ch. 240)

(62) Palatine, lateral ramus shape: plate-shaped (long maxillary contact) (0); rod-shaped (narrow maxillary contact) (1). ([S29]:ch. 40)

(63) Epipterygoid: present (0); absent (1). ([S29]:ch. 41)

(64) Vomer, anterior articulation: maxilla (0); premaxilla (1). ([S29]:ch. 42)

(65) Supraoccipital, height: twice subequal to (0); or less than height of foramen magnum (1). ([S29]:ch. 43)

(66) Paroccipital process, ventral non-articular process: absent (0); present (1). ([S29]:ch. 44)

(67) Crista prootica, size: rudimentary (0); expanded laterally into dorsolateral process (1). ([S29]:ch. 45)

(68) Basipterygoid processes, length: short, approximately twice (0); or elongate, at least four times basal diameter (1). ([S29]:ch. 46)

(69) Basipterygoid processes, angle of divergence: approximately 45° (0); less than 30° (1). ([S29]:ch. 47)

(70) Basal tubera, anteroposterior depth: approximately half dorsoventral height (0); sheetlike, 20% dorsoventral height (1). ([S29]:ch. 48)

(71) Basal tubera, breadth: much broader than (0); or narrower than occipital condyle (1). ([S29]:ch. 49)

(72) Basal tubera: distinct from basipterygoid (0); reduced to slight swelling on ventral surface of basipterygoid (1). ([S45]:ch. 53)

(73) Basal tubera, shape of posterior face: convex (0); slightly concave (1). ([S45]:ch. 54)

(74) Basioccipital depression between foramen magnum and basal tubera: absent (0); present (1). ([S29]:ch. 50)

(75) Basisphenoid/basipterygoid recess: present (0); absent (1). ([S29]:ch. 51)

(76) Basisphenoid/quadrate contact: absent (0); present (1). ([S29])

(77) Basisphenoid, sagital ridge between basipterygoid processes: absent (0); present (1). ([S46]:ch. 242)

(78) Basipterygoid processes, orientation: perpendicular to (0); or angled approximately 45° to skull roof (1). ([S29]:ch. 53)

(79) Basipterygoid, area between the basipterygoid processes and parasphenoid rostrum: is a mildly concave subtriangular region (0); forms a deep slot-like cavity that passes posteriorly between the bases of the basipterygoid processes (1). ([S50]:ch. 48)

(80) Occipital region of skull, shape: anteroposteriorly deep, paroccipital processes oriented posterolaterally (0); flat, paroccipital processes oriented transversely (1). ([S29]:ch. 54)

(81) Dentary, depth of anterior end of ramus: slightly less than that of dentary at midlength (0); 150% minimum depth (1). ([S29]:ch. 55)

(82) Dentary, anteroventral margin shape: gently rounded (0); sharply projecting triangular process (1). ([S29]:ch. 56)

(83) Dentary symphysis, orientation: angled 15° or more anteriorly to (0); or perpendicular to axis of jaw ramus (1). ([S29]:ch. 57)

(84) Dentary, cross-sectional shape of symphysis: oblong or rectangular (0); subtriangular, tapering sharply towards ventral extreme (1); subcircular (2). ([S45]:ch. 60)

(85) Dentary, tuberocity on labial surface near symphysis: absent (0); present (1). ([S45]:ch. 57)

(86) Mandible, coronoid eminence: strongly expressed, clearly rising above plane of dentigerous portion (0); absent (1). ([S45]:ch. 62)

(87) External mandibular fenestra: present (0); absent (1). ([S29]:ch. 58)

(88) Surangular depth: less than twice (0); or more than two and one-half times maximum depth of the angular (1). ([S29]:ch. 59)

(89) Surangular ridge separating adductor and articular fossae: absent (0); present (1). ([S29]:ch. 60)

(90) Adductor fossa, medial wall depth: shallow (0); deep, prearticular expanded dorsoventrally (1). ([S29]:ch. 61)

(91) Splenial posterior process, position: overlapping angular (0); separating anterior

portions of prearticular and angular (1). ([S29]:ch. 62)

(92) Splenial posterodorsal process: present, approaching margin of adductor chamber (0); absent (1). ([S29]:ch. 63)

(93) Coronoid, size: extending to dorsal margin of jaw (0); reduced, not extending dorsal to splenial (1); absent (2). ([S29]:ch. 64)

(94) Tooth rows, shape of anterior portions: narrowly arched, anterior portion of tooth rows V-shaped (0); broadly arched, anterior portion of tooth rows U-shaped (1); rectangular, tooth-bearing portion of jaw perpendicular to jaw rami (2). ([S29]:ch. 65)

(95) Tooth rows, length: extending to orbit (0); restricted anterior to orbit (1); restricted anterior to antorbital fenestra (2); restricted anterior to subnarial foramen (3). (Modified from [S29]:ch. 66). **Ordered**.

(96) Dentary teeth, number: greater than 20 (0); 10-17 (1); 9 or fewer (2). (modified from [S29]:ch.73). **Ordered**.

(97) Replacement teeth per alveolus, number: two or fewer (0); more than four (1). ([S29]:ch. 74)

(98) Lateral plate: absent (0); present (1). ([S48]:ch. 9)

(99) Teeth, orientation: perpendicular (0); or oriented anteriorly relative to jaw margin (1). ([S29]:ch. 75)

(100) Tooth crowns, orientation: aligned along jaw axis, crowns do not overlap (0); aligned slightly anterolingually, tooth crowns overlap (1). ([S29]:ch. 69)

(101) Crown-to-crown occlusion: absent (0); present (1). ([S29]:ch. 67)

(102) V-shaped wear facets: present (0); absent (1). (Modified from [S29]:ch. 68)

(103) Tooth crowns, cross-sectional shape at mid-crown: elliptical (0); D-shaped (1); subcylindrical (2); cylindrical (3). ([S29]:ch. 70)

(104) Enamel surface texture: entirely smooth (0); finely wrinkled in some patches (1); extensively and coarsely wrinkled (2) ([S29]: ch. 117).

(105) Thickness of enamel asymmetric labiolingually: absent (0); present (1). ([S45]:ch. 74)

(106) Marginal tooth denticles: present (0); absent on posterior edge (1); absent on both anterior and posterior edges (2). ([S29]:ch. 72). **Ordered**.

(107) Teeth, longitudinal grooves on lingual aspect: absent (0); present (1). ([S29]:ch. 76)

(108) SI values for tooth crowns: less than 3.0 (0); 3.0-4.0 (1); 4.0-5.0 (2); more than 5.0 (3). ([S48]:chs. 67-69). **Ordered**.

(109) Cervical vertebrae, number: 10 or fewer (0); 12 (1); 13-14 (2); 15 (3); 16 or more (4). (Modified from [S29]:ch. 80 and [S48]:chs. 96-100).

(110) Atlas, intercentrum occipital facet shape: rectangular in lateral view, length of dorsal aspect subequal to that of ventral aspect (0); expanded anteroventrally in lateral view, anteroposterior length of dorsal aspect shorter than that of ventral aspect (1). ([S29]:ch. 79).

(111) Cervical centra, articulations: amphicoelous (0); opisthocoelous (1). ([S29]:ch. 82)

(112) Cervical centra, ventral surface: is flat or slightly convex transversely (0); transversely concave (1). ([S48]:ch. 107)

(113) Cervical centra, midline keels on ventral surface: prominent and plate-like (0); reduced to low ridges or absent (1). ([S48]:ch. 106)

(114) Cervical centra, pleurocoels: absent (0); present with well defined anterior, dorsal, and ventral edges, but not the posterior one (1); present, with well defined edges; present but very reduced in size (3). ([S47])

(115) Cervical centra, pleurocoels: singles without division (0); with a well defined anterior excavation and a posterior smooth fossa (1); divided by a bone septum, resulting in an anterior and a posterior lateral excavation (2); divided in three or more lateral excavations, resulting in a complex morphology (3); with a well defined anterior excavation and a posterior smooth fossa (Modified from [S51]; [S29]; [S52])**. Ordered.**

(116) Cervical vertebrae, height divided width (measured in its posterior articular surface): higher than 1.1 (0), around 1 (1); between 0.9 and 0.7 (2); smaller than 0.7 (3). (Modified from [S29]:ch. 84; [S48]:ch. 108)**. Ordered.**

(117) Cervical centra, small notch in the dorsal margin of the posterior articular surface:
absent (0); present (1). ([S47])

(118) Cervical vertebrae, neural arch lamination: well developed, with well marked laminae and fossae (0); rudimentary, with diapophyseal laminae absents or very slightly marked (1). ([S29]:ch, 81)

(119) Cervical vertebrae with an accessory lamina, which runs from the postzygodiapophyseal lamina (PODL) up to the spinoprezygapophyseal lamina (SPRL): absent (0); present (1). (Modified from [S53]:chs. 50, 51; [S45]:chs. 78, 96).

(120) Cervical centra, internal pneumaticity: absent (0); present with singles and wide cavities (1); present, with several small and complex internal cavities (2). (Modified from [S54])**. Ordered.**

(121) Anterior cervical vertebrae, prespinal lamina: absent (0); present (1). ([S47]).

(122) Anterior cervical vertebrae, neural spine shape: single (0); bifid (1). ([S29]:ch. 72; [S48]:ch. 118)

(123) Middle and posterior cervical vertebrae, prespinal lamina: absent (0); present (1). ([S47]).

(124) Middle cervical vertebrae, lateral fossae on the prezygapophysis process: absent (0); present (1). ([S52]).

(125)Middle, cervical vertebrae, height of the neural arch: less than the height of the posterior articular surface (0); higher than the height of the posterior articular surface (1). ([S29]:ch. 87; similar [S48]:111 and 112)

(126)Middle cervical centrum, anteroposterior length divided the height of the posterior articular surface: less than 4 (0); more than 4 (1). ([S29]:ch. 74; and [S48]:ch. 102).

(127) Middle and posterior cervical vertebrae, morphology of the centroprezygapophyseal lamina: single (0); dorsally divided, resulting in a lateral and medial lamina, being the medial lamina linked with the intraprezygapophyseal lamina and not with the prezygapophysis (1); divided, resulting in the presence of a “true” divided centroprezygapophyseal lamina, which is dorsally connected to the prezygapophisis (2). ([S47]).

(128) Middle and posterior cervical vertebrae, morphology of the centropostzygapophyseal lamina (CPOL): single (0); divided, with the medial part contacting the intrapostzygapophyseal lamina (1) ([S47])

(129) Middle and posterior cervical vertebrae, articular surface of zygapophyses: flat (0); transversally convex (1). ([S48])

(130) Posterior cervical vertebrae, lateral profile of the neural spine: displays steeply sloping cranial and caudal faces (0); displays steeply sloping cranial face and noticeably less steep caudal margin (1). ([S48]:ch. 119)

(131) Posterior cervical vertebrae, neural spine shape: without a great lateral expansion (0); laterally expanded, being equal or wider than the vertebral centrum (1). ([S55])

(132) Posterior cervical and anterior dorsal vertebrae, neural spine shape: single (0); bifid (1). ([S29]:ch. 90, [S48]:ch. 118)

(133) Posterior cervical and anterior dorsal bifid neural spines, median tubercle: absent (0); present (1).

(134) Number of dorsal vertebrae: 14 or more (0); 13 (1); 12 (2); 10 (3). (Modified from [S29]:ch. 91; [S48]:ch. 122-125)

(135) Dorsal centra, pleurocoels: absent (0); present (1). ([S29]:ch. 78; [S48]:128)

(136) Dorsal vertebrae, transverse processes: are directed laterally or slightly upwards (0); are directed strongly dorsolaterally (1). ([S48]:ch. 138)

(137) Dorsal vertebrae, distal end of the transverse process: curves smoothly into the dorsal surface of the process (0); is set off from the dorsal surface, the latter having a distinct dorsally facing flattened area (1). ([S48]:ch. 140)

(138) Dorsal vertebrae, non bifid neural spine in anterior or posterior view: posses subparallel lateral margins (0); posses lateral margins which slightly diverge dorsally (1); posses lateral margins which strongly diverge dorsally (2). (Modified from [S29]:ch. 107; [S48]:ch. 155)

(139) Dorsal centra, pneumatic structures: absent, dorsal centra with solid interna structure (0); present, dorsal centra with simple and big air-spaces (camerate) (1); present, dorsal centra with small and complex air-spaces (polycamerate) (2); present, dorsal centra with small and complex air spaces (semicamellate/camellate) (3). (Modified from [S54])

(140) Anterior and middle dorsal neural spines, spinoprezygapophyseal lamina (SPRL): absent (0); present (1).(Modified from [S56]:ch. 131).

(141) Posterior dorsal neural spines, spinoprezygapophyseal lamina (SPRL): absent (0); present (1). (Modified from [S56]:ch. 132).

(142) Dorsal vertebrae, single not bifid neural spines, single prespinal lamina (PRSL): absent (0); present (1). (Modified from [S51]:ch.14)

(143) Dorsal vertebrae, single not bifid neural spines, single prespinal lamina (PRSL): rough and wide, present in the dorsalmost part of the neural spine (0); rough and wide, extended trough almost all the neural spine (1); smooth and narrow (2). ([S47])

(144) Dorsal vertebrae with single neural spines, middle single fossa projected trought the middline of the neural spine: present (0); absent (1). ([S47])

(145) Dorsal vertebrae with single neural spines, middle single fossa, projected through the midline of the neural spine: relatively wide median simple fossa (0); a thin median simple fossa (1); extremely reduced median simple fossa (2). ([S47])**.**

Ordered.

(146) Anterior dorsal centra, articular face shape: amphicoelous (0); opisthocoelous (1). ([S29]:ch. 94; [S48]:ch. 104)

(147) Anterior and middle dorsal centra, pleurocoels: have rounded caudal margins (0); have tapering, acute caudal margins (1). ([S51]; [S48]:ca 127)

(148)Middle dorsal neural arches in lateral view, anterior edge of the neural spine: project anteriorly to the diapophysis (0); converge with the diapophysis (1); project posteriorly to the diapophysis (2). ([S47])

(149) Anterior and middle dorsal vertebrae, zygapophyseal articulation angle: horizontal or slightly posteromedially oriented (0); posteromedially oriented (around 30º) (1); strongly posteroventraly oriented (more than 40º) (2). ([S47])

(150) Middle to posterior dorsal centra, ventral surface: convex transversely (0); flattened (1); is slightly concave, sometimes with one or two crests (2). ([S48])

(151) Middle dorsal vertebrae, hyposphene-hypantrum system: present (0); absent (1). (Modified from [S51]:ch. 25; [S29]:ch. 106; [S48]:ch. 145)

(152) Posterior dorsal vertebrae, hyposphene-hypantrum system: present and well developed, usually with a rhomboid shape (0); present and weakly developed, mainly as a laminar articulation (1); absent or only present in posteriormost dorsal vertebrae (2). ([S47])**. Ordered.**

(153) Middle and posterior dorsal vertebrae, transverse processes length: short (0); long (projecting along 1.5 the articular surface width) (1). ([S47])

(154) Mid and posterior dorsal vertebrae with a single lamina (the single TPOL) supporting the hyposphene or postzygapophysis from below: absent (0); present (1). (Modified from [S48]:ch. 146)

(155) Middle and posterior dorsal vertebrae, neural canal in anterior view: entirely surrounded by the neural arch (0); enclosed in a deep fossa, enclosed laterally by pedicels (1). ([S48]:ch. 136)

(156) Middle and posterior dorsal vertebrae, neural spine height: approximately twice the centrum length (0); for times the centrum length (1). ([S48])

(157) Middle and posterior dorsal neural spines orientation: vertical (0); slightly inclined, with an angle of around 70 degrees (1); strongly inclined, with an angle not bigger than 40 degrees (2). (Modified from [S29]:ch. 104)

(158) Middle and posterior dorsal neural arches, centropostzygapophyseal lamina (CPOL), shape: simple (0); divided (1). ([S29]:ch. 95)

(159) Middle and posterior dorsal neural arches, anterior centroparapophyseal lamina (ACPL): absent (0); present (1). ([S29]:ch. 96; [S48]:ch. 133)

(160) Middle and posterior dorsal neural arches, prezygoparapophyseal lamina (PRPL): absent (0); present (1). ([S29]:ch. 97)

(161) Middle and posterior dorsal neural arches, posterior centroparapophyseal lamina (PCPL): absent (0); present (1). ([S29]:ch. 98, [S48]:ch. 137)

(162) Middle and posterior dorsal centrum in transverse section (height: width ratio): subcircular (ratio, similar to 1 or a bit higher) (0); slightly dorsoventrally compressed (ratios between 0.8 and 1) (1); strongly compressed (ratios below 0.8) (2). (Modified from [S48])

(163) Middle and posterior dorsal vertebrae neural spine, triangular aliform processes: absent (0); present but do not project far laterally (not as far as caudal zygapophyses) (1); present and

project far laterally (as far as caudal zygapophyses) (2). (Modified from [S29]:ch. 102 and [S48]:chs. 153-154)**. Ordered.**

(164) Middle and posterior dorsal vertebrae, spinodiapophyseal lamina (SPDL): absent (0); present (1). ([S48]:ch. 157)

(165) Middle and posterior dorsal vertebrae, accessory spinodiapophyseal lamina: absent (0); present (1). ([S48]:ch. 151)

(166) Dorsal vertebrae, spinodiapophyseal webbing: lamina follows curvature of neural spine in anterior view (0); lamina "festooned" from spine, dorsal margin does not closely follow shape of neural spine and diapophysis (1). ([S45]:ch.104)

(167) Anterior dorsal vertebrae, spinopostzygapophyseal lamina (SPOL): absent (0); present (1). ([S56]:ch.133)

(168) Middle and posterior dorsal neural spines, lateral spinopostzygapophyseal lamina (lSPOL): absent (0); present (1). ([S29]: 100; [S48]:ch. 159)

(169) Middle and posterior dorsal neural arches, spinodiapophyseal lamina (SPDL) and spinopostzygapophyseal lamina (lSPOL) contact: absent (0); present (1). ([S29]:ch. 101)

(170) Middle and posterior dorsal vertebrae, spinodiapophyseal (SPDL) and spinopostzygapophyseal lamina (lSPOL) contact: ventral, well separated from the triangular aliform process (0); dorsal, forms part of the triangular aliform process (1). ([S47])

(171) Middle and posterior dorsal vertebrae, height of neural arch below the postzygapophyses (pedicel): less than height of centrum (0); subequal to or greater than height of centrum (1). ([S45]:ch. 109)

(172) Posterior Dorsal vertebrae, medial spinopostzygapophyseal lamina (mSPOL): absent (0); present and forms part of the median posterior lamina (1). ([S47])

(173) Posterior dorsal vertebrae, transverse processes: lie posterior, or posterodorsal, to the parapophysis (0); lie vertically above the parapophysis (1). ([S48]:ch. 139)

(174) Posterior dorsal centra, articular face shape: amphicoelous (0); slightly opisthocoelous (1); opisthocoelous (2). (Modified from [S29]:ch. 105)

(175) Posterior dorsal vertebrae, neural spine: narrower transversely than anteroposteriorly (0); broader transversely than anteroposteriorly (1). ([S29]: ch. 92)

(176) Posterior dorsal vertebra, posterior centrodiapophyseal lamina (PCDL): has an unexpanded ventral tip (0); expands and may bifurcate toward its ventral tip (1). ([S51])

(177) Cervical ribs, distal shafts of longest cervical ribs: are elongate and form overlapping bundles (0); are short and do not project beyond the caudal end of the centrum to which they are attached (1). ([S29]:ch. 140)

(178) Cervical ribs, angle between the capitulum and tuberculum: greater than 90°, so that the rib shaft lies close to the ventral edge of the centrum (0); less than 90°, so that the rib shaft lies below the ventral margin of the centrum (1). ([S29]:ch. 139)

(179) Dorsal ribs, proximal pneumatopores: absent (0); present (1). ([S29]:ch. 141)

(180) Anterior dorsal ribs, cross-sectional shape: subcircular (0); plank-like, anteroposterior breadth more than three times mediolateral breadth (1). ([S29]).

(181) Sacral vertebrae, number:: 3 or fewer (0); 4 (1); 5 (2); 6 (3). ([S29]:ch. 108)

(182) Sacrum, sacricostal yoke: absent (0); present (1). ([S29]:ch. 109)

(183) Sacral vertebrae contributing to acetabulum: numbers 1-3 (0); numbers 2-4 (1). ([S29]:ch. 110)

(184) Sacral neural spines length: approximately twice length of centrum (0); approximately four times length of centrum (1). ([S29]:ch. 111)

(185) Sacral ribs, dorsoventral length: low, not projecting beyond dorsal margin of ilium (0); high extending beyond dorsal margin of ilium (1). ([S29]:ch. 112)

(186) Pleurocoels in the lateral surfaces of sacral centra: absent (0); present (1). ([S48]:ch. 165)

(187) Caudal vertebrae, number: 35 or fewer (0); 40 to 55 (1); increased to 70-80 (2). ([S29]:ch.114)

(188) Caudal bone texture: solid (0); spongy, with large internal cells (1). ([S29]:ch. 113)

(189) Caudal transverse processes: persist through caudal 20 or more posteriorly (0); disappear by caudal 15 (1); disappear by caudal 10(2). ([S29]:ch. 115)

(190) First caudal centrum or last sacral vertebra, articular face shape: flat (0); procoelous (1); opisthocoelous (2); biconvex (3). ([S29])

(191) First caudal neural arch, coel on lateral aspect of neural spine: absent (0); present (1). ([S29]:ch. 117)

(192) Anterior caudal vertebrae, transverse processes: ventral surface directed laterally or slightly ventrally (0); directed dorsally (1). ([S45]:ch. 125)

(193) Anterior caudal centra (excluding the first), articular face shape: amphiplatyan or amphicoelous (0); procoelous/distoplatyan (1); slightly procoelous (2); procoelous (3); posterior surface markedly more concave than the anterior one (4). (Modified from [S55])

(194) Anterior caudal centra, pleurocoels: absent (0); present (1). ([S29]:ch. 119)

(195) Anterior caudal vertebrae, ventral surfaces: convex transversely (0); concave transversely (1). ([S48]:ch. 182)

(196) Anterior and middle caudal vertebrae, ventrolateral ridges: absent (0); present (1). ([S48]:ch. 183)

(197) Anterior and middle caudal vertebrae, triangular lateral process on the neural spine: absent (0); present (1). ([S45]:ch. 123)

(198) Anterior caudal transverse processes shape: triangular, tapering distally (0); "wing-like",not tapering distally (1). ([S29]:ch. 128)

(199) Anterior caudal neural spines, transverse breadth: approximately 50% of (0); or greater than anteroposterior length (1). ([S29]:ch. 126)

(200) Anterior caudal transverse processes, proximal depth: shallow, on centrum only (0); deep, extending from centrum to neural arch (1). ([S29]:ch. 127)

(201) Anterior caudal transverse processes, diapophyseal laminae (ACDl, PCDL, PRDL, PODL): absent (0); present (1). ([S29]:ch. 129)

(202) Anterior caudal transverse processes, anterior centrodiapophyseal lamina (ACDL), shape: single (0); divided (1). ([S29]:ch. 130)

(203) Anterior caudal vertebrae, hyposphene ridge: absent (0); present (1). ([S48]:ch. 187)

(204) Anterior caudal centra, length: approximately the same (0); or doubling over the first 20 vertebrae (1). ([S29]:ch. 120)

(205) Anterior caudal neural arches, spinoprezygapophyseal lamina (SPRL): absent, or present as small short ridges that rapidly fade out into the anterolateral margin of the spine (0); present, extending onto lateral aspect of neural spine (1). (Modified from [S29]:ch. 121)

(206) Anterior caudal neural arches, spinoprezygapophyseal lamina (SPRL)-spinopostzygapophyseal lamina (SPOL) contact: absent (0); present, forming a prominent lamina on lateral aspect of neural spine (1). ([S29]:ch. 122)

(207) Anterior caudal neural arches, prespinal lamina (PRSL): absent (0); present (1). ([S29]:ch. 123)

(208) Middle caudal centra, shape: cylindrical (0); with flat ventral margin (1); quadrangular, flat ventrally and laterally (2). (Modified from [S29]:ch. 131)

(209) Anterior and middle caudal centra, ventral longitudinal hollow: absent (0); present (1). ([S29]:ch. 132)

(210) Middle caudal centra, articular face shape: amphiplatyan or amphicoelous (0); procoelous/distoplatyan (1); slightly procoelous (2); procoelous (3). ([S55])

(211) Middle caudal vertebrae, location of the neural arches: over the midpoint of the centrum with approximately subequal amounts of the centrum exposed at either end (0); on the anterior half of the centrum (1). ([S48]:ch. 185)

(212) Middle caudal vertebrae, height of the pedicels below the prezygapophysis: low with curved anterior edge of the pedicel (0); high with vertical anterior edge of the pedicel (1). ([S47])

(213) Middle caudal vertebrae, orientation of the neural spines: anteriorly (0); vertical (1); slightly directed posteriorly (2); strongly directed posteriorly (3). (Modified from [S29]:ch. 133)**. Ordered.**

(214) Posterior caudal vertebrae, neural spine strongly displacced posteriorly: absent (0); present (1). ([S47]).

(215)Middle caudal vertebrae, ratio of centrum length to centrum height: less than 2, usually 1.5 or less (0); 2 or higher (1). ([S48]:ch. 179)

(216) Anterior-posterior caudal vertebrae (those with still well developed neural spine), neural spine orientation: vertical (0); slightly directed posteriorly (1); strongly directed posteriorly (2). ([S47])**. Ordered.**

(217) Posterior Caudals centra, articular face shape: anphyplatic (0); procoelous (1); opisthocoelous (2). (Modified from [S55])

(218) Posterior caudal centra, shape: cylindrical (0); dorsoventrally flattened, breadth at least twice height (1). ([S29]:ch. 135)

(219) Posterior caudal vertebrae, ratio of length to height: less than 5, usually 3 or less (0); 5 or higher (1). ([S48]:ch. 180)

(220) Distalmost caudal centra, articular face shape: platycoelous (0); biconvex (1). ([S29]:ch. 136)

(221) Distalmost biconvex caudal centra, number: 10 or fewer (0); more than 30 (1). ([S29]:ch. 137)

(222) Distalmost biconvex caudal centra, length-to height ratio: less than 4 (0); greater than 5 (1). ([S29]:ch. 138)

(223) Forked chevrons with anterior and posterior projections: absent (0); present (1). ([S29]:ch. 143)

(224) Forked chevrons, distribution: distal tail only (0); throughout middle and posterior caudal vertebrae (1). ([S29]:ch. 144)

(225) Chevrons, crus bridging dorsal margin of haemal canal: present (0); absent (1). ([S29]:ch. 145)

(226) Chevron haemal canal, depth: short, approximately 25% (0); or long, approximately 50% chevron length (1). ([S29]:ch. 146)

(227) Chevrons: persisting throughout at least 80% of tail (0); disappearing by caudal 30 (1). ([S29]:ch. 147)

(228) Posterior chevrons, distal contact: fused (0); unfused (open) (1). ([S29]:ch. 148)

(229) Posture: bipedal (0); columnar, obligatory quadrupedal posture (1). ([S29]:ch. 149)

(230) Scapular acromion process, size: Narrow (0); broad, width more than 150% minimum width of blade (1). ([S29]:ch. 150)

(231) Scapular blade, orientation respect to coracoid articulation: perpendicular (0); forming a 45º angle (1). ([S29]:ch. 151)

(232) Scapular blade, shape: acromial edge not expanded (0); rounded expansion on acromial side (1); racquet-shaped (2). ([S29]:ch. 152). **Ordered**.

(233) Scapula, acromion process dorsal margin: concave or straight (0); with V-shaped concavity (1); with U-shaped concavity (2). ([S53]: 88). **Ordered**.

(234) Scapula, highest point of the dorsal margin of the blade: lower than the dorsal margin of the proximal end (0); at the same height than the dorsal margin of the proximal end (1); higher than the dorsal margin of the proximal end (2). ([S47] from [S57]). **Ordered**.

(235) Scapula, development of the acromion process: undeveloped (0); well developed (1). ([S47])

(236) Scapular length/minimum blade breadth: 5.5 or leas (0); 5.5 or more (1). ([S47])

(237) Scapula, ventral margin with a well developed ventro medial process: absent (0); present (1). ([S54])

(238) Scapular, acromial process position: lies nearly glenoid level (0); lies nearly midpoint scapular body (1). ([S47])

(239) Scapular acromion length: less than 1/2 scapular length (0); at least 1/2 scapular length (1). ([S50]: ch. 168)

(240) Glenoid scapular orientation: relatively flat or laterally facing (0); strongly beveled medially (1). ([S29]:ch. 153)

(241) Scapular blade, cross-sectional shape at base: flat or rectangular (0); D-shaped (1). ([S29]:ch. 154)

(242) Coracoid, proximodistal length: less than the length of scapular articulation (0); approximately twice the length of scapular articulation (1). ([S29]:ch. 155)

(243) Coracoid, anteroventral margin shape: rounded (0); rectangular (1). ([S29]:ch. 156)

(244) Dorsal margin of the coracoid in lateral view: reaches or surpasses the the level of the dorsal margin of the scapular expansion (0); lies below the level of the scapular proximal expansion and separated from the latter by a V-shaped notch (1). ([S48]:ch. 207)

(245) Coracoid, Infraglenoid deep groove: absent (0); present (1).

(246) Coracoid, infraglenoid lip: absent (0); present (1). ([S29]:ch. 157)

(247) Sternal plate, shape: oval (0); crescentic (1). ([S29]:ch. 158)

(248) Prominent posterolateral expansion of the sternal plate producing a kidney-shaped profile in dorsal view: absent (0); present (1). ([S48]:ch.211)

(249) Prominent parasagital oriented ridge on the dorsal surface of the sternal plate: absent (0); present (1). ([S48]: ch.212)

(250) Ridge on the ventral surface of the sternal plate: absent (0); present (1). ([S48]:ch.213)

(251) Ratio of maximum length of sternal plate to the humerus length: less than 0,75, usually less than 0,65 (0); greater than 0,75 (1). ([S48]:ch.209)

(252) Humerus-to-femur ratio: less than 0.60 (0); 0.60 to 0.90 (1); greater than 0.90 (2). ([S48]:ch. 216). **Ordered**.

(253) Humeral deltopectoral attachment, development: prominent (0); reduced to a low crest or ridge (1). ([S29]:ch.160)

(254) Humeral deltopectoral crest, shape: relatively narrow throughout length (0); markedly expanded distally (1). ([S29]:ch.161)

(255) Humeral midshaft cross-section, shape: circular (0); elliptical (1). ([S58]:ch. 170)

(256) Humerus, RI: Gracile (less than 0,27) (0); medium (0,28-0,32) (1); Robust (more than 0,33) (2). ([S47]). **Ordered** character.

(257) Humeral distal condyles, articular surface shape: restricted to distal portion of humerus (0); exposed on anterior portion of humeral shaft (1). ([S29]:ch. 163)

(258) Humeral distal condyle, shape: divided (0); flat (1). ([S29]:ch. 164)

(259) Humeral, lateral margin: medially deflected (0); almost straight until the half length or even more (1). ([S47])

(260) Humeral proximolateral corner, shape: rounded, the dorsal surface is well convex (0); pronounced / square, the dorsal surface low, almost flat (1). ([S29]:ch. 159)

(261) Ulnar proximal condyle, shape: subtriangular (0); triradiate, with deep radial fossa (1). ([S29]ch. 165)

(262) Ulnar proximal condylar processes, relative lengths: subequal (0); unequal, anterior arm longer (1). ([S29]:ch. 166)

(263) Ulnar olecranon process, development: prominent, projecting above proximal articulation (0); rudimentary, level with proximal articulation (1). ([S29]: ch. 167)

(264) Ulna, length-to-proximal breadth ratio: gracile (0); stout (1). ([S29]:ch. 168)

(265) Radial distal condyle, shape: round (0); subrectangular, flattened posteriorly and articulating in front of ulna (1). ([S29]:ch. 169)

(266) Radius, distal breadth: slightly larger than midshaft breadth (0); approximately twice midshaft breadth (1). ([S29]:ch.170)

(267) Radius, distal condyle orientation: perpendicular to long axis of shaft (0); beveled approximately 20º proximolaterally relative to long axis of shaft (1). ([S29]:ch.171)

(268) Carpal bones, number: 3 or more (0); 2 or fewer (1). ([S29]:ch.173)

(269) Carpal bones, shape: round (0); block-shaped, with flattened proximal and distal surfaces (1). ([S29]:ch.174)

(270) Metacarpus, shape: spreading (0); bound, with subparallel shafts and articular surfaces that extend half their length (1). ([S29]:ch.175)

(271) Metacarpals, shape of proximal surface in articulation: gently curving, forming a 90arc (0); U-shaped, subtending a 270arc (1). ([S29]:ch.176)

(272) Longest metacarpal-to-radius ratio: close to 0.3 (0); 0.45 or more (1). ([S29]:ch.177)

(273) Metacarpal I, length: shorter than metacarpal IV (0); longer than metacarpal IV (1). ([S29]:ch.178)

(274) Metacarpal I, distal condyle shape: divided (0); undivided (1). ([S29]:ch. 179)

(275) Metacarpal I distal condyle, transverse axis orientation: beveled approximately 20º respect to axis of shaft (0); proximodistally or perpendicular with respect to axis of shaft (1). ([S29]:ch. 180)

(276) Manual digits II and III, phalangeal number: 2- 3-4-3-2 or more (0); reduced, 2-2-2-2-2 or less (1); absent or unossified (2). ([S29]:ch. 181)

(277) Manual phalanx I.1, shape: rectangular (0); wedge-shaped (1). ([S29]:ch. 182)

(278) Manual nonungual phalanges, shape: longer proximodistally than broad transversely (0); broader transversely than long proximodistally (1). ([S29]:ch. 183)

(279) Pelvis, anterior breadth: narrow, ilia longer anteroposteriorly than distance separating preacetabular processes (0); broad, distance between preacetabular processes exceeds anteroposterior length of ilia (1). ([S29]:ch. 1842)

(280) Ilium, ischial peduncle size: large, prominent (0); low, rounded (1). ([S29]:ch. 185)

(281) Ilium, dorsal margin shape: flat (0); semicircular (1). ([S29]:ch. 186)

(282) Ilium, preacetabular process shape: pointed, arching ventrally (0); semicircular, with posteroventral excursion of cartilage cap (1). ([S29]:ch. 188)

(283) Ilium, preacetabular process orientation: anterolateral to body axis (0); perpendicular to body axis (1). ([S29]:ch. 189)

(284) Highest point on the dorsal margin of the ilium: lies caudal to the base of the pubic process (0); lies cranial to the base of the pubic process (1). ([S48]:ch. 245)

(285) Pubis length respect to ischium: pubis slightly smaller or subequal to ischium (0); pubis larger (120% +) than ischium (1). ([S47])

(286) Pubis, ambiens process development: small, confluent with anterior margin of pubis prominent, (0); projects anteriorly from anterior margin of pubis (1). ([S29]:ch. 189)

(287) Pubic apron, shape: flat (straight symphysis) (0); canted anteromedially (gentle Sshaped symphysis) (1). ([S29]:ch. 190).

(288) Puboischial contact, length: approximately one third total length of pubis (0); one-half total length of pubis (1). ([S29]:ch. 191)

(289) Ischium, acetabular articular surface: maintains approximately the same transverse width throughout its length (0); is transversely narrower in its central portion and strongly expanded as it approaches the iliac and pubic articulations (1). ([S50]:ch. 180)

(290) Ischium, iliac peduncle with constriction or "neck": absent (0); present (1). ([S45]:ch. 173).

(291) Ischium, elongate muscle scar on proximal end: absent (0); present (1). ([S45]:ch. 174)

(292) Ischial blade, shape: emarginate distal to pubic peduncle (0); no emargination distal to pubic peduncle (1). ([S29]:ch. 193)

(293) Ischia pubic articulation: less or equal to the anteroposterior length of pubic pedicel (0); greater than the anteroposterior length of pubic pedicel (1). ([S51])

(294) Ischia, anteroposterior pubic pedicel width divided the total length of the ischium: less than 0,5 (0); 0,5 or grate (1); Large (2). ([S47]).

(295) Ischial distal shaft, shape: triangular, depth of ischial shaft increases medially (0); bladelike, medial and lateral depths subequal (1). ([S48]:ch. 194)

(296) Ischial distal shafts, cross-sectional shape: V-shaped, forming an angle of nearly 50º with each other (0); flat, nearly coplanar (1). ([S29]:ch. 195)

(297) Ischia, distal end: is only slightly expanded (0); is strongly expanded dorsoventrally (1). ([S59]:ch. 183)

(298) Ichium, angle formed between the shaft and the acetabular line: forming an almost right angle (80-110°) (0) or; a close angle (less than 70°) (1). ([S47])

(299) Femur, fourth trochanter development: prominent (0); reduced to crest or ridge (1); extremely reduced (2). (Modified from [S29]:ch. 196, following to [S45]:ch. 186). **Ordered**.

(300) Femur, lesser trochanter: present (0); absent (1). ([S29]:ch. 197)

(301) Femur midshaft, transverse diameter: subequal to anteroposterior diameter (0); 125- 150% anteroposterior diameter (1); at least 185% anteroposterior diameter (2). ([S29]:ch. 198). **Ordered**.

(302) Femur, lateral bulge (marked by the lateral expansion and a dorsomedial orientation of the laterodorsal margin of the femur, which starts below the femur head ventral margin): absent (0); present (1). ([S51])

(303) Femur, pronounced ridge on posterior surface between greater trochanter and head: absent (0); present (1). ([S45]:ch. 181)

(304) Femur head position: perpendicular to the shaft, rises at the same level than the greater trochanter (0); dorsally directed, rises well above the level of the greater trochanter (1). (Modified from [S48]:ch. 263)

(305) Femur, distal condyles relative transverse breadth: subequal (0); tibial much broader than fibular (1). ([S29]:ch. 2000)

(306) Femur, distal condyles orientation: perpendicular or slightly beveled dorsolaterally (0); or beveled dorsomedially approximately 10 relative to femoral shaft (1). ([S29]:ch. 201)

(307) Femur, distal condyles articular surface shape: restricted to distal portion of femur (0); expanded onto anterior portion of femoral shaft (1). ([S29]:ch. 202)

(308) Situation of the femoral fourth trochanter: on the caudal surface of the shaft, near the midline (0); on the caudomedial margin of the shaft (1). ([S48]:ch. 268)

(309) Tibial proximal condyle, shape: narrow, long axis anteroposterior (0); expanded transversely, condyle subcircular (1). ([S29]:ch. 203)

(310) Tibial cnemial crest, orientation: projecting anteriorly (0); or laterally (1). ([S29]:ch. 204)

(311) Tibia, distal breadth: approximately 125% (0); more than twice midshaft breadth (1). ([S29]:ch. 205)

(312) Tibial distal posteroventral process, size: broad transversely, covering posterior fossa of astragalus (0); shortened transversely, posterior fossa of astragalus visible posteriorly (1). ([S29]:ch. 206)

(313) Fibula, proximal tibial scar, development: not well-marked (0); well-marked and deepening anteriorly (1). ([S29]:ch. 207)

(314) Fibula, lateral trochanter: absent (0); present (1). ([S29]:ch. 208)

(315) Fibular distal condyle, size: subequal to shaft (0); expanded transversely, more than twice midshaft breadth (1). ([S29]:ch. 209)

(316) Astragalus, shape: rectangular (0); wedge shaped, with reduced anteromedial corner (1). ([S29]:ch.210)

(317) Astragalus, fibular facet: faces laterally (0); faces posterolaterally, anterior margin visible in posterior view (1). ([S45]:ch. 186)

(318) Astragalus, foramina at base of ascending process: present (0); absent (1). ([S29]:ch. 211)

(319) Astragalus, ascending process length: limited to anterior two-thirds of astragalus (0); extending to posterior margin of astragalus (1). ([S29]:ch. 212)

(320) Astragalus, posterior fossa shape: undivided (0); divided by vertical crest (1). ([S29]:ch. 213)

(321) Astragalus, transverse length: 50% more than (0); or subequal to proximodistal height (1). ([S29]:ch. 214)

(322) Calcaneum: present (0); absent or unossified (1). ([S29]:ch. 215)

(323) Distal tarsals 3 and 4: present (0); absent or unossified (1). ([S29]:ch. 216)

(324) Metatarsus, posture: bound (0); spreading (1). ([S29]:ch. 217)

(325) Metatarsal I proximal condyle, transverse axis orientation: perpendicular to (0); angled ventromedially approximately 15º to axis of shaft (1). ([S29]:ch. 218)

(326)Metatarsal I distal condyle, transverse axis orientation: perpendicular to (0); angled dorsomedially to axis of shaft (1). ([S29]:ch. 219)

(327)Metatarsal I distal condyle, posterolateral projection: absent (0); present (1). ([S29]:ch. 220)

(328) Metatarsal I, minimum shaft width: less than that of metatarsals IIIV (0); or greater than that of metatarsals IIIV (1). ([S29]:ch. 221)

(329) Metatarsal I and V proximal condyle, size: smaller than (0); or subequal to those of metatarsals II and IV (1). ([S29]:ch. 222)

(330) Metatarsal III length: more than 30% (0); or less than 25% that of tibia (1). ([S29]:ch. 223)

(331) Metatarsals III and IV, minimum transverse shaft diameters: subequal to (0); or less than 65% that of metatarsals I or II (1). ([S29]:ch. 224)

(332) Metatarsal V, length: shorter than (0); or at least 70% length of metatarsal IV (1). ([S29]:ch. 225)

(333) Pedal nonungual phalanges, shape: longer proximodistally than broad transversely (0); broader transversely than long proximodistally (1). ([S29]:ch. 226)

(334) Pedal digits II-IV, penultimate phalanges, development: subequal in size to more proximal phalanges (0); rudimentary or absent (1). ([S29]:ch. 227)

(335) Pedal unguals, orientation: aligned with (0); or deflected lateral to digit axis (1). ([S29]:ch. 228)

(336) Pedal digit I ungual, length relative to pedaldigit II ungual: subequal (0); 25% larger than that of digit II (1). ([S29]:ch. 229)

(337) Pedal digit I ungual, length: shorter (0); or longer than metatarsal I (1). ([S29]:ch. 230)

(338) Pedal ungual I, shape: broader transversely than dorsoventrally (0); sickle-shaped, much deeper dorsoventrally than broad transversely (1). ([S29]:ch. 231)

(339) Pedal ungual IIIII, shape: broader transversely than dorsoventrally (0); sickle-shaped, much deeper dorsoventrally than broad transversely (1). ([S29]:ch. 232)

(340) Pedal digit IV ungual, development: subequal in size to unguals of pedal digits II and III (0); rudimentary or absent (1). ([S29]:ch. 233)

(341) Unguals of pedal digit II and III, proximal dimensions: as broad as deep (0); significantly broader than deep (1). ([S26]:ch. 253)

(342) Development of v-shaped wear facets: well developed (forming “shoulders”) (0); slightly developed as marginal facets (1).

(343) Single planar wear facet on labial or lingual surface of teeth: absent (0); present (1).

(344) One high angled wear facet and a second low angle wear facet: absent (0); present (1).

(345) Tooth crown shape: narrow crowns (0); broad crowns (1).

(346) Middle to posterior dorsal vertebrae, pleurocoel dorsal margin: rounded (0) angular (1).

(347) Middle to posterior dorsal vertebrae, peurocoel dorsal margin: well below the dorsal margin of the centrum (0) at the level of the dorsal margin of the centrum or higher (1).

(348) Middle to posterior dorsal vertebrae, small fossa anterior to anteroventral to the pleurocoel: absent (0) present (1)

(349) Premaxilla-maxilla suture, shape: planar (0) twisted along its length, giving the contact a sinuous appearance in lateral view (1). ([S60]:ch. 2)

(350) Premaxilla, small finger-like, vertically oriented premaxillary process near anteromedial corner of external naris: absent (0); present (1). ([S60]:ch. 3)

(351) Dentary, posteroventral process shape: single (0) divided (1). ([S60]:ch. 10)

(352) Maxillary teeth, shape: straigth along axis (0); twisted axially through an arc of 30-45º (1). ([S60]:ch. 15)

(353) Axis, centrum shape: over two and a half times as long as tall (0); less than twice as long as tall (1). ([S60]:ch. 20)

(354) Cervical vertebrae, epipophyses shape: stout, pillar-like expansions above postzygapophyses (0); posteriorly projecting prongs (1). ([S60]:ch. 24)

(355) Middle and posterior cervical vertebrae, parapophyses shape: subcircular (0); elongate (1). ([S60]:ch. 28)

(356) Middle and posterior dorsal vertebral centra, ventral keel: absent (0); present (1). ([S60]:ch. 49)

(357) Anterior caudal vertebrae (mainly the first and second): ventral bulge on transverse process: absent (0); present (1). ([S60]:ch. 52)

(358) Anterior and middle caudal vertebrae, blind fossae in lateral centrum: absent (0); present (1). ([S60]:ch. 56)

(359)Middle caudal vertebrae, transverse processes orientation: perpendicular (0); swept backwards, reaching the posterior margin of the centrum (1). ([S60]:ch. 59)

(360) Sternal plate, shape: posterolateral margin curved (0); posterolateral margin expanded as a corner (1). ([S60]:ch. 76)

(361) Humerus, strong posterolateral bulge on around level of the deltopectoral crest: absent (0); present (1). ([S60]:ch. 80)

(362) Humerus, radial and ulnar condyles, shape: radial condyle divided on anterior face by a notch (0); undivided (1). ([S60]:ch. 83)

(363) Ilium, preacetabular process, kink on ventral margin: absent (0); present (1). ([S60]:ch. 99)

(364) Femur, longitudinal ridge on anterior face: absent (0); present (1). ([S60]:ch. 107)

(365) Fibula, proximal end, anterior crest: absent or poorly developed (0); well developed creating interlocking proximal cruz (1). ([S60]:ch. 111)

(366) Fibula, shaft shape: straight, or sligthly sigmoidal (0); sigmoid, such that the proximal and distal faces are angled relative to midshaft (1). ([S60]:ch. 113)

(367) Astragalus, shape: at least 1.5 times wider than anteroposteriorly long (0); anteroposterior and transverse dimensions subequal (1). ([S60]:ch. 115)

(368) Metatarsal IV, proximomedial end, shape: flat or slightly concave (0); possesses a distinct embayment (1). ([S60]:ch. 117)

(369) Metatarsal IV, distal end, orientation: roughly perpendicular to long axis of bone (0); bevelled upwards medially (1). ([S60]:ch. 118)

(370) Foramen magnum: vertically taller than wide transversely (0); wider than tall (1); sub equal measures. (modified from [S61]:ch. 333)

(371) Supraoccipital: vertically taller than transversaly wide (0); wider than tall (1). ([S61]:ch. 337).

(372) Contribution of supraoccipital to the margin of foramen magnum: more than 10% the entire margin or more than 50% the dorsal margin (0); less than 10% the entire margin or less than 50% the dorsal margin due to medially expanded exoccipitals (1). ([S61]:ch. 338).

(373) Craniopharingeal foramen position: posterior to basal basal tubera (0); anterior to basal tubera (1). ([S61]:ch. 343).

(374) Cervical diapophyses, prominent triangular flange on caudal edge of diapophyseal process, absent (0); present (1). ([S62]: ch 78).

(375) Cervical prezygapophyses, cranial process situated ventrolaterally to articular surface, absent (0); present (1). ([S62]: ch 79).

(376) Middle cervical vertebrae, dorsoventral height of neural spine respect to height of the centra: lower (0); slightly lower or same (1); highest (2).

(377) Middle cervical vertebrae, prezygapophysis position: do not extend beyond the anterior margin of centrum (0); extend beyond the anterior margin of the centrum (1)

(378) Shape of the external naris (in adults): rounded (0) or subtriangular with an acute posteroventral corner (1). ([S29]: ch 17).

(379) Nasal relationship with dorsal margin of antorbital fossa: not contributing to the margin of the antorbital fossa (0), lateral margin overhangs the antorbital fossa and forms its dorsal margin (1), overhang extensive, obscuring the dorsal lachrymal−maxilla contact in lateral view (2). ([S29]: ch 23).

(380) Shape of the antorbital fossa: crescentic with a strongly concave posterior margin that is roughly parallel to the rostral margin of the antorbital fossa (0), subtriangular with a straight to gently concave posterior margin (1), or antorbital fossa absent (2). ([S29]: ch 32).

(381) Length of the quadratojugal ramus of the squamosal relative to the width at its base: less than (0), or greater than (1), four times its width. ([S29]: ch 61).

(382) Shape of upper jaws in ventral view: narrow with an acute rostral apex (0) or broad and U-shaped (1). ([S29]: ch 95).

(383) Lingual concavities of the teeth: absent (0) or present (1). ([S29]: ch 118).

(384) Longitudinal labial grooves on the teeth: absent (0) or present (1). ([S29]: ch 119).

(385) Distribution of the serrations along the mesial and distal carinae of the tooth: extend along most of the length of the crown (0) or are restricted to the upper half of the crown (1). ([S29]: ch 120).

(386) Lateral compression of the anterior cervical vertebrae: centra are no higher than they are wide (0) or are approximately 1.25 times higher than wide (1). ([S29]: ch 130).

(387) Separation of lateral surfaces of anterior dorsal neural arches under transverse processes: widely spaced (0) or only separated by a thin midline septum (1). ([S29]: ch 163).

(388) Height of dorsal neural arches, from neurocentral suture to level of zygapophyseal facets: much less than (0), or subequal to or greater than (1), height of centrum. ([S29]: ch 164).

(389) Shape of posterior dorsal neural canal: subcircular (0) or slit-shaped (1). ([S29]: ch 166).

(390) Well-developed, sheet-like suprapostzygapophyseal laminae: absent (0), present on at least the caudal dorsal vertebrae (1). ([S29]: ch 171).

(391) Caudal margin of the acromion process of the scapula: rises from the blade at angle that is less than (0), or greater than (1), 65° from the long axis of the scapula at its steepest point. ([S29]: ch 201).

(392) Flat, caudoventrally facing surface on the coracoid between glenoid and coracoid tubercle: absent (0) or present (1). ([S29]: ch 203).

(393) Transverse width of the distal humerus: is less than (0), or greater than (1), 33% of the length of the humerus. ([S29]: ch 211).

(394) Shape of the distal ends of second and third metacarpals: subrectangular in distal view (0) or trapezoidal with flexor rims of distal collateral ligament pits flaring beyond extensor rims (1). ([S29]: ch 230).

(395) Ventrolateral twisting of the transverse axis of the distal end of the first phalanx of manual digit one relative to its proximal end: absent (0), present but much less than 60° (1), or 60° (2). ([S29]: ch 234).

(396) Length of the postacetabular process of the ilium: between 40 and 100% of the distance between the pubic and ischial peduncles (0), less than 40% of this distance (1), or more than 100% of this distance (2). ([S29]: ch 255).

(397) Minimum transverse width of the pubic apron: much more than (0), or less than (1), 40% of the width across the iliac peduncles of the ilium. ([S29]: ch 262).

(398) Ischial component of acetabular rim: larger than (0), or equal to (1), the pubic component. ([S29]: ch 273).

(399) Depth of the transverse section of the ischial shaft: much less than (0), or at least as great as (1), the transverse width of the section. ([S29]: ch 276).

(400) Shape of the cross-section of the midshaft of the femur: subcircular (0) or strongly elliptical with the long axis orientated mediolaterally (1). ([S29]: ch 281).

(401) Shape of femoral head: roughly rectangular in profile with a sharp medial distal corner (0) or roughly hemispherical with no sharp medial distal corner (1). ([S29]: ch 283).

(402) Position of the lesser trochanter: near the centre of the anterior face (0), or close to the lateral margin (1), of the femoral shaft in anterior view. ([S29]: ch 290).

(403) Visibility of the lesser trochanter in posterior view: not visible (0) or visible (1). ([S29]: ch 291).

(404) Position of the fourth trochanter along the length of the femur: in the proximal half (0) or straddling the midpoint (1). ([S29]: ch 293).

(405) Symmetry of the profile of the fourth trochanter of the femur: subsymmetrical without a sharp distal corner (0) or asymmetrical with a steeper distal slope than the proximal slope and a distinct distal corner (1). ([S29]: ch 294).

(406) Shape of the anteromedial corner of the distal articular surface of the tibia: forming a right angle (0) or forming an acute angle (1). ([S29]: ch 310).

(407) Depth of the medial end of the astragalar body in cranial view: roughly equal to the lateral end (0) or much shallower, creating a wedgeshaped astragalar body (1). ([S29]: ch 315).

(408) Shape of the posteromedial margin of the astragalus in dorsal view: forming a moderately sharp corner of a subrectangular astragalus (0) or evenly rounded without formation of a caudomedial corner (1). ([S29]: ch 316).

(409) Transverse width of the calcaneum: greater than (0), or less than (1), 30% of the transverse width of the astragalus. ([S29]: ch 324).

(410) Pedal digit five: reduced, nonweight bearing (0) or large (fifth metatarsal at least 70% of fourth metatarsal), robust and weight bearing (1). ([S29]: ch 341).

(411) Shape of the unguals of pedal digits two and three: dorsoventrally deep with a proximal articulating surface that is at least as deep as it is wide (0) or dorsoventrally flattened with a proximal articulating surface that is wider than deep (1). ([S29]: ch 348).

(412) Posterior margin of astragalus: straight (0) or convex (1). ([S29]: ch 362).

Added Characters

(413) Occipital condyle, lateral surface of the basioccipital: flat or slightly convex (0); strongly concave (1). ([S62]: ch 50).

(414) Occipital condyle, an angle with respect to the supraoccipital plane: less than 100 degrees (0); more than 100 degrees (1). ([S61]:ch. 332).

(415) A vertical ridge extending from the postorbital contact of the laterosphenoid along the frontal-parietal suture dorsally and eventually reaching the posterolateral corner of the frontal: bsent (0); present (1). ([S61]:ch. 334).

(416) Transverse distance between right and left laterosphenoid-postorbital contacts: nearly equal to the distance between the lateral tips of posterior lateral wings of the parietal (0); approximately 25% narrower than transverse distance between the (1). ([S61]:ch. 335).

(417) Frontoparietal fenestra: absent (0); present (1). ([S63]:ch. 36)

(418) Frontoparietal fenestra: enclosed within parietals (0); incorporates frontals (1). ([S61]:ch. 336).

(419) Supraoccipital ridge: transversally narrow (0); transversally robust (1); robust with a knob near the skull roof (2). ([S61]:ch. 339).

(420) The height of parietal along the supraoccipital-parietal suture: more than the height of exoccipital along supraoccipital-exoccipital suture (0); approximately equal to the height of exoccipital along supraoccipital-exoccipital suture (1); less than the height of exoccipital along supraoccipital-exoccipital suture (2). ([S61]:ch. 340).

(421) External foramen for trigeminal nerve (CN V): posterior to crista antotica (0); directly below or anterior to crista antotica (1). ([S61]:ch. 341).

(422) Crista interfenestralis: Absent (0); incipient (1); nearly or entirely separating the fenestra ovalis and the metotic fissure (2). ([S61]:ch. 342).

(423) (Craniopharyngeal foramen) Basisphenoid fossa/foramen between foramen magnum and basal tubercula: absent (0); present (1) ([S61]:ch. 73).

(424) Craniopharyngeal foramen: does not form a notch that separates the basal tubera from each other (0); forms a notch that separates the basal tubera from each other (1). ([S61]:ch. 344).

(425) Dorsal vertebrae, height of the neural arch divided the height of the centrum: less than 0.8 (0); more than 0.8 (1). (Modified from [S63]: ch. 132)

(426) Size and position of the posterolateral process of premaxilla: large and lateral to the anterior process of the maxilla (0) or small and medial to the anterior process of the maxilla (1). ([S29]: ch 7).

(427) Shape of the anteromedial process of the maxilla: narrow, elongated, and projecting anterior to lateral premaxilla−maxilla suture (0) or short, broad, and level with lateral premaxilla−maxilla suture (1). ([S29]: ch 10).

(428) Development of external narial fossa: absent to weak (0) or well developed with sharp posterior and anteroventral rims (1). ([S29]: ch 11).

(429) Development of narial fossa on the anterior ramus of the maxilla: weak and orientated laterally to dorsolaterally (0) or well developed and forming a horizontal shelf (1). ([S29]: ch 12).

(430) Shape of subnarial foramen: rounded (0) or slot-shaped (1). ([S29]: ch 14).

(431) Level of the posterior margin of external naris: anterior to, or level with, the premaxilla−maxilla suture (0), posterior to the first maxillary alveolus (1), or posterior to the midlength of the maxillary tooth row and the anterior margin of the antorbital fenestra (2). ([S29]: ch 19).

(432) Length of rostral ramus of the maxilla: less than (0), or greater than (1), its dorsoventral depth. ([S29]: ch 26).

(433) Direction that the neurovascular foramen at the caudal end of the lateral maxillary row opens: caudally (0) or rostrally, ventrally, or laterally (1). ([S29]: ch 34).

(434) Dorsal exposure of the lachrymal: present (0) or absent (1). ([S29]: ch 37).

(435) Orientation of the lachrymal orbital margin: strongly sloping anterodorsally (0) or erect and close to vertical (1). ([S29]: ch 39).

(436) Extension of the antorbital fossa onto the ventral end of the lachrymal: present (0) or absent (1). ([S29]: ch 42).

(437) Shape of the suborbital region of the jugal: an anteroposteriorly elongate bar (0) or an anteroposteriorly shortened plate (1). ([S29]: ch 49).

(438) Position of the rostral margin of the infratemporal fenestra: behind the orbit (0), extends under the rear half of the orbit (1), or extends as far forward as the midlength of the orbit (2). ([S29]: ch 57).

(439) Length of jugal ramus of quadratojugal: no longer than (0), or longer than (1), the squamosal ramus. ([S29]: ch 65).

(440) Shape of the rostral end of the jugal ramus of the quadratojugal: tapered (0) or dorsoventrally expanded (1). ([S29]: ch 66).

(441) Medial process of the pterygoid forming a hook around the basipterygoid process: absent (0), flat and blunt-ended (1), or bent upward and pointed (2). ([S29]: ch 92).

(442) Splenial foramen: absent (0), present and enclosed (1), or present and open anteriorly (2). ([S29]: ch 102).

(443) Length of the axial centrum: less than (0), or at least (1), three times the height of the centrum. ([S29]: ch 126).

(444) Postzygodiapophyseal lamina in cervical neural arches 4-8: present (0), or absent (1). ([S29]: ch 142).

(445) Ventral surface of the centra in the cervicodorsal transition: transversely rounded (0) or with longitudinal keels (1). ([S29]: ch 145).

(446) Form of anterior surface of neural arch: simple centroprezygapophyseal ridge (0) or broad anteriorly facing surface bounded laterally by centroprezygapophyseal lamina (1). ([S29]: ch 165).

(447) Shape of posterior margin of middle dorsal neural spines in lateral view: approximately straight (0) or concave with a projecting posterodorsal corner (1). ([S29]: ch 173).

(448) Length of the radius: greater than (0), or less than (1), 80% of the length of the humerus. ([S29]: ch 213).

(449) Deep radial fossa, bounded by an anterolateral process, on proximal ulna: absent (0) or present but poorly defined (1), or a well-defined recess, deeper than the transverse wifth of the anterior end of the anterior process (2). (Modified from [S9] by [S64]). **Ordered**.

(450) Lateral end of first distal carpal: abuts (0), or overlaps (1), second distal carpal. ([S29]: ch 219).

(451) Proximal end of first metacarpal: flush with other metacarpals (0) or inset into the carpus (1). ([S29]: ch 226).

(452) Length of the fifth metacarpal: less than (0), or greater than (1), 75% of the length of the third metacarpal. ([S29]: ch 232).

(453) Shape of the proximal articular surface of the first phalanx of manual digit one: rounded (0) or with an embayment on the medial side (1). ([S29]: ch 236).

(454) Shape of the first phalanx of manual digit one: elongate and subcylindrical (0) or strongly proximodistally compressed and wedge-shaped (1). ([S29]: ch 237).

(455) Length of the ungual of manual digit two: greater than the length of the ungual of manual digit one (0), 75–100% of the ungual of manual digit one (1), less than 75% of the ungual of manual digit one (2), or the ungual of manual digit two is absent (3). ([S29]: ch 242).

(456) Phalangeal formula of manual digits two and three: three and four, respectively (0), or with at least one phalanx missing from each digit (1). ([S29]: ch 243).

(457) Cranial extent of preacetabular process of ilium: does not (0), or does (1), project further forward than cranial end of the pubic peduncle. ([S29]: ch 246).

(458)Depth of the preacetabular process of the ilium: much less than (0), or subequal to (1), the depth of the ilium above the acetabulum. ([S29]: ch 248).

(459) Width of the conjoined pubes: less than (0), or greater than (1), 75% of their length. ([S29]: ch 259).

(460) Orientation of the entire blades of the pubic apron: transverse (0) or twisted posteromedially (1). ([S29]: ch 266).

(461) Shape of the lesser trochanter: small rounded tubercle (0), proximodistally orientated, elongate ridge (1), or absent (2). ([S29]: ch 285).

(462) Position of proximal tip of lesser trochanter: level with (0), or distal to (1), the femoral head. ([S29]: ch 286).

(463) Position of the tallest point of the cnemial crest: close to the proximal end of the crest (0) or about half-way along the length of the crest, creating an anterodorsally sloping proximal margin of the crest (1). ([S29]: ch 302).

(464) A triangular rugose area on the medial side of the fibula: absent (0) or present (1). ([S29]: ch 312).

(465) Ossified distal tarsals: present (0) or absent (1). ([S29]: ch 330).

(466) Transverse width of the proximal end of the fourth metatarsal: less than (0), or at least (1), twice the anteroposterior depth of the proximal end. ([S29]: ch 338).

(467) Shape of the lateral margin of the proximal surface of the second metatarsal: straight (0) or concave (1). ([S29]: ch 335).

(468) Length of nonterminal pedal phalanges: all longer than wide (0), proximal-most phalanges longer than wide whereas more distal phalanges are as wide as long (1), or all nonterminal phalanges are as wide, if not wider, than long (2). ([S29]: ch 342).

(469) Shape of proximal articular surface of pedal unguals: proximally facing, visible on medial and lateral sides (0) or proximomedially facing and visible only in medial view, causing medial deflection of pedal unguals in articulation (1). ([S29]: ch 346).

(470) Number of phalanges in pedal digit four: four (0) or fewer than four (1). ([S29]: ch 351).

(471) Distal articular surface of astragalus: relatively flat or weakly convex (0) or extremely convex and roller-shaped (1). ([S29]: ch 355).

(472) Distal surface of tibiofibular crest: as deep anteroposteriorly as wide mediolaterally or deeper (0) or wider mediolaterally than deep anteroposteriorly (1). ([S29]: ch 356).

(473) Profile of the distal articular surface of astragalus in anterior or posterior views: straight (0), concave (1), or convex (2). (Modified from [S29]: ch 364).

(474) Biceps tubercle of the radius: absent (0) or present (1). ([S29]: ch 368).

(475) Position of the ventral margin of the anterior process of the lacrimal: close to the proximal end (0); or close to the half of the dorsoventral length (1). (**This contribution**)

(476) Caudal end of dentary tooth row medially inset with a thick lateral ridge on the dentary forming a buccal emargination: absent (0) or present (1) ([S29]: ch 97).

(477) Shallow, dorsally facing fossa on the atlantal neurapophysis bordered by a dorsally everted lateral margin: absent (0) or present (1) ([S29]: ch 122).

(478) Minimum transverse shaft width of first metacarpal: less than (0), or greater than (1), twice the minimum transverse shaft width of second metacarpal ([S29]: ch 225).

(479) Development of the antorbital fossa on the ascending ramus of the maxilla: deeply impressed and delimited by a sharp, scarp-like rim (0) or weakly impressed and delimited by a rounded rim or a change in slope (1) ([S29]: ch 31).

(480) Shape of the dorsal margin of postorbital in lateral view: straight to gently curved (0) or with a distinct embayment between the anterior and posterior dorsal processes (1). ([S29]: ch 54).

(481) Notch separating posteroventral end of the ischial obturator plate from the ischial shaft: present (0) or absent (1) ([S29]: ch 268).

(482) Dorsal profile of the snout: straight to gently convex (0) or with a depression behind the naris (1). ([S29]: ch 20).

(483) Web of bone spanning junction between anterior and ventral rami of lachrymal: absent and antorbital fossa laterally exposed (0) or present, obscuring posterodorsal corner of antorbital fossa (1) ([S29]: ch 41).

(484) Position of foramina for midcerebral vein on occiput: between supraoccipital and parietal (0) or on the supraoccipital (1) ([S29]: ch 73).

(485) Lateral extent of ventrolateral flange on plantar surface of metatarsal II in proximal aspect: similar in development to ventromedial flange (0) or well developed, extending further laterally tan ventromedial flange extends medially (1) ([S29]: ch 354).

(486) Proximal outline of metatarsal III: subtriangular with acute or rounded posterior border (0) or subtrapezoidal, with posterior border broadly exposed in plantar view (1) ([S29]: ch 358).

(487) Length of the first phalanx of manual digit one: less than (0), or greater than (1), the length of the first metacarpal ([S29]: ch 235).

(488) Shape of the caudal margin of the postacetabular process of the ilium: rounded to bluntly pointed (0), square-ended (1), or with a pointed ventral corner and a rounded caudodorsal margin (2) ([S29]: ch 258). **Unordered**.

(489) Position of jaw joint: no lower than the level of the dorsal margin of the dentary (0) or depressed well below this level (1) ([S29]: ch 94).

(490) Shape of posteromedial heel of distal tarsal four (lateral distal tarsal): proximodistally deepest part of the bone (0) or no deeper than the rest of the bone (1) ([S29]: ch 328).

(491) Shape of the floor of the braincase in lateral view: relatively straight with the basal tuberae, basipterygoid processes, and parasphenoid rostrum roughly aligned (0), bent with the basipterygoid processes and the parasphenoid rostrum below the level of the basioccipital condyle and the basal tuberae (1), or bent with the basal tuberae lowered below the level of the basioccipital and the parasphenoid rostrum raised above it (2) ([S29]: ch 81). **Unordered**.

(492) Length of the manus: less than 38% (0), 38– 45% (1), or greater than 45% (2), of the humerus + radius ([S29]: ch 222). **Ordered**.

(493) Length of the deltopectoral crest of the humerus: less than 30% (0), 30–50% (1), or greater than 50% (2), of the length of the humerus ([S29]: ch 207). **Ordered**.

(494) Length of manual digit one: less than (0), or greater than (1), the length of manual digit two ([S29]: ch 233).

(495) Longitudinal axis of the femur in lateral view: strongly bent with an offset between the proximal and distal axes greater than 15° (0), weakly bent with an offset of less than 10° (1), or straight ([S65). **Ordered**.

(496) Width of dorsal expansion of the scapula: less than (0), or equal to (1), the width of the ventral end of the scapula ([S45]).

(497) Shape of the first metacarpal: proximal width less than 65% (0), 65–80% (1), 80–100% (2), or greater than 100% (3), of its length ([S29]: ch 227).

(498) Height of middle dorsal neural spines: less than the length of the base (0), higher than the than 1.5 times the length of the base (2) ([S29]: ch 267). **Ordered.**

(499) Anterior tip of anterior process of proximal ulna: no deflection or continues lateral curvature (0), medially deflected (1) ([S30]: ch 218).

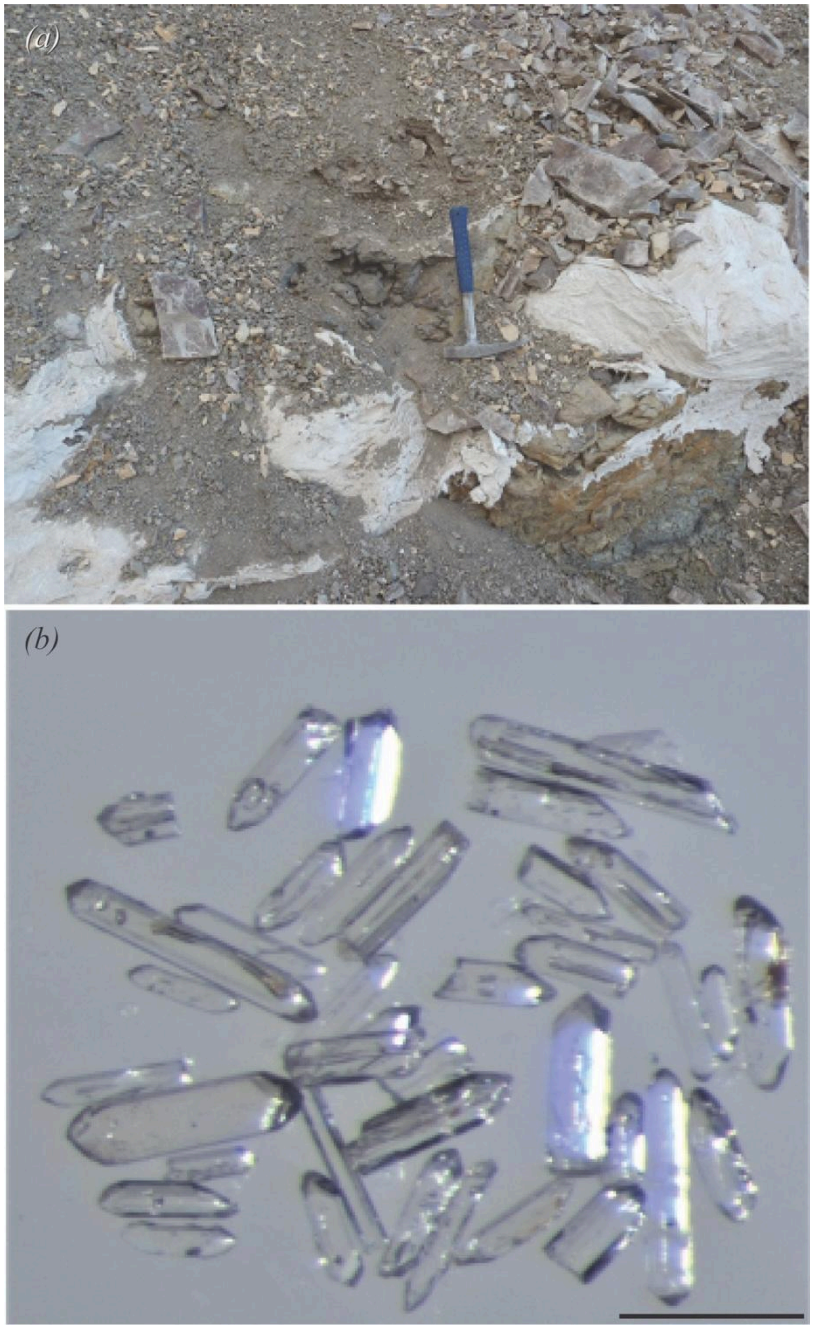

Figure S1. (*a*) Outcrop photograph of the sampled tuff (adjacent to rock hammer) from the *Bagualia alba* bone bed within the lower strata of the Cañadón Asfalto Formation. **(*b*)** Microscope image of separated zircons from tuff sample CA041412-2. Scale bar, 200 μm.

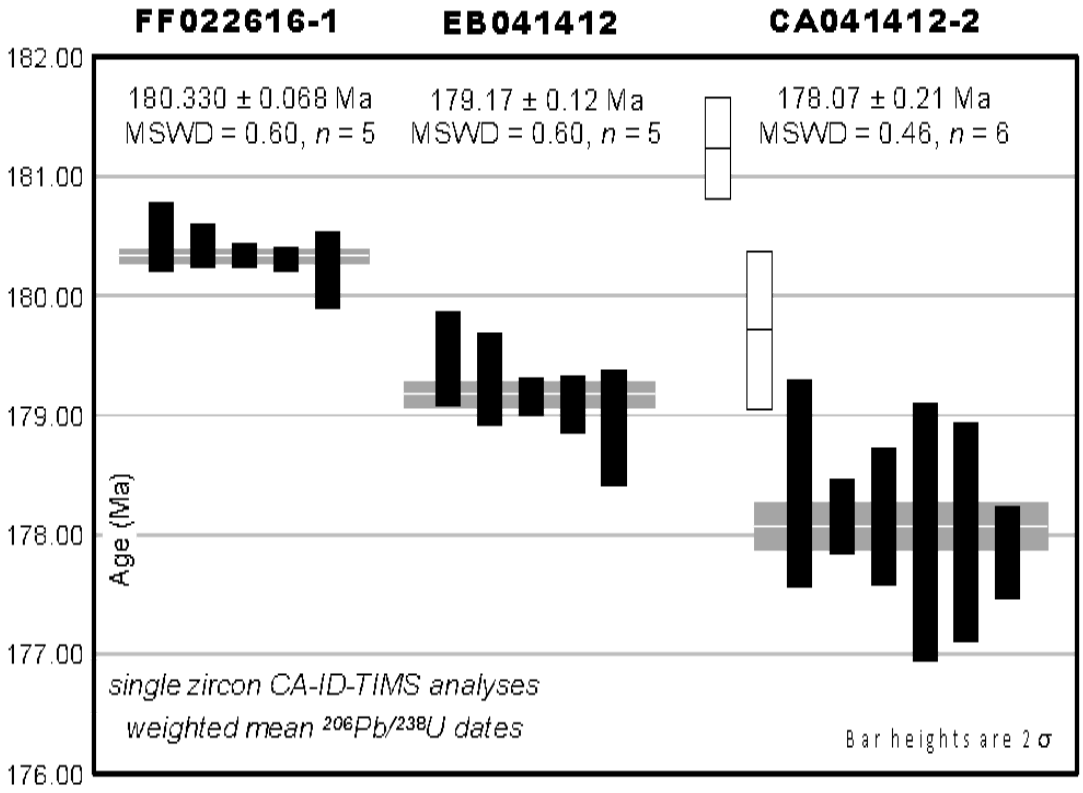

Figure S2. Date distribution plot of zircon CA-ID-TIMS U-Pb analyzes from Cañadón Asfalto basin tuff samples. Solid bars are individual zircon analyses. Horizontal shaded band represents the weighted mean $^{206}Pb/^{238}U$ date and its 95% confidence level internal uncertainty. See Data S2 for complete U-Pb data.

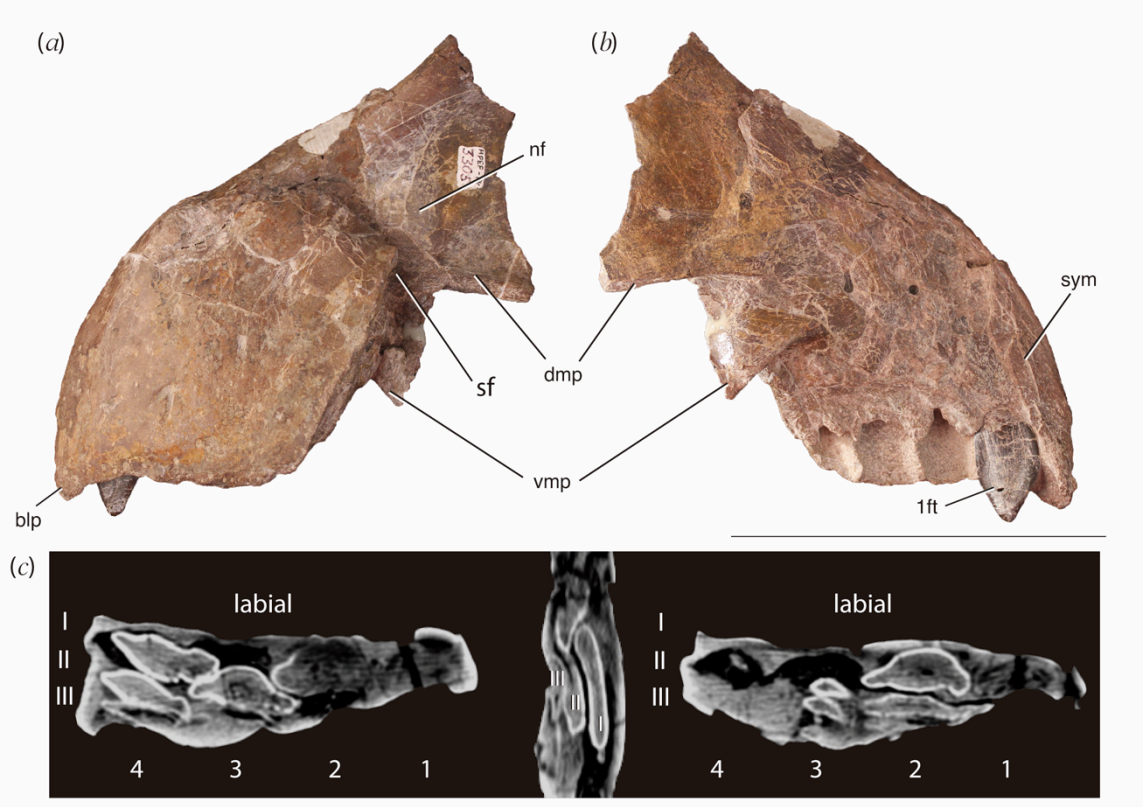

Fig. S3. Left premaxilla (MPEF-PV 3305). (***a***) Lateral view. (***b***) Medial view. (***c***) CT images in transverse and sagittal sections. Scale bar, 10 cm. blp, beak like process; dmp, dorsomedial process; nf, narial fossa; sf, subnarial foramen; sym, symphysis; vmp, ventromedial process; 1ft, first functional tooth; 1-4, alveolus position; I-III, replacement tooth position in each of the four alveoli.

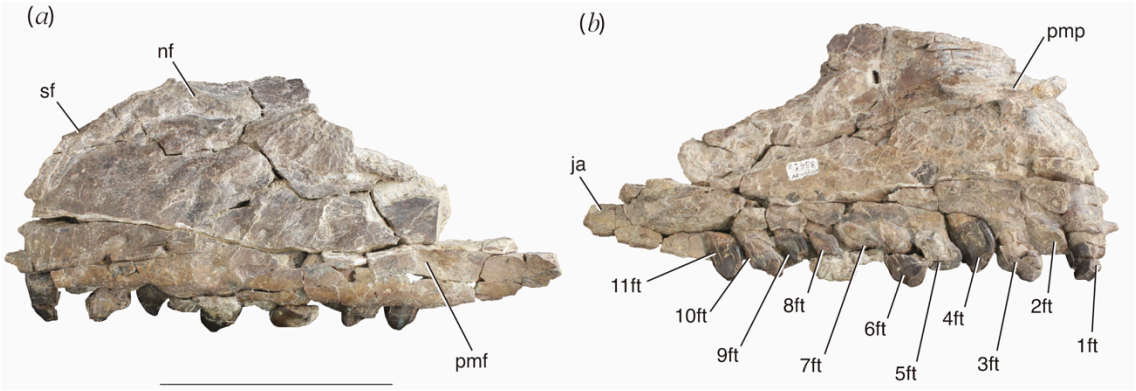

Fig. S4. Left maxilla (MPEF-PV 33041a). (***a***) lateral view. (***b***) Medial view. Scale bar, 10 cm. ja, jugal articulation; nf, narial fossa; pmf, posterior maxillary foramen; pmp, premaxillary process; sf, subnarial foramen; 1ft-11ft, functional teeth from 1 to 11.

Fig. S5. Frontals (MPEF-PV 3301-3). Scale bar, 5 cm. in, indentation; la, lacrimal articulation; na, articular facet for nasal; o, orbit; pa, parietal articulation; poa, articular facet for postorbital; prfa, articular facet for prefrontal.

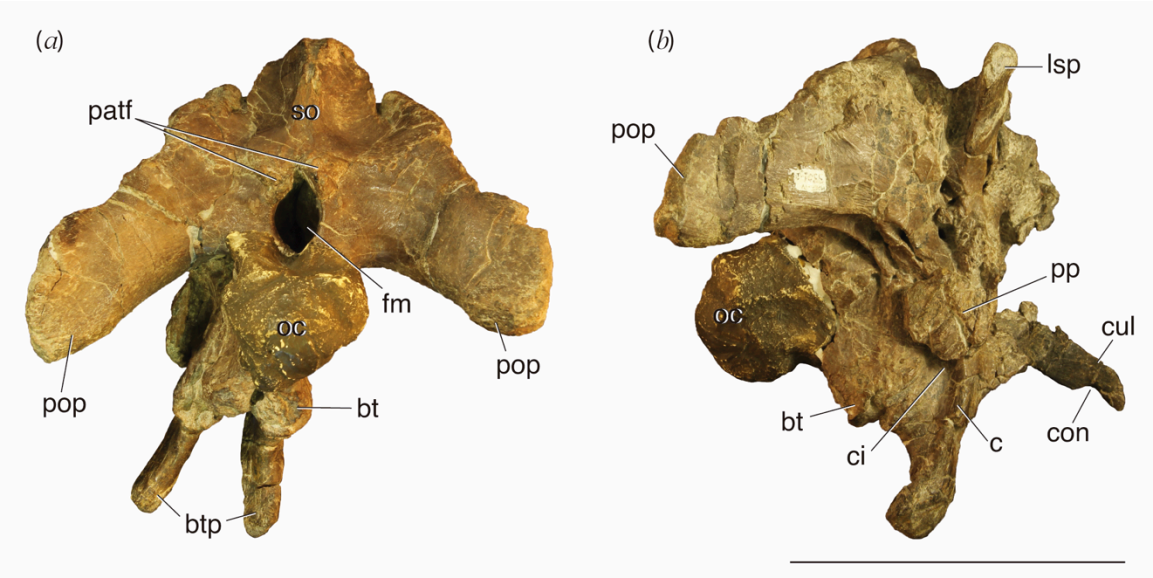

Fig. S6. Braincase (MPEF-PV 3301-1). Scale bar, 10 cm. bt, basal tuber; btp, basipterygoid process; c, crest; ci, entrance of the internal carotid artery; con, concavity; cul, cultriform process; fm, foramen magnum, lsp, laterosphenoid; oc, occipital condyle; patf, proatlantal facet; pop, paroccipital process; pp, preotic pendant; so, supraoccipital.

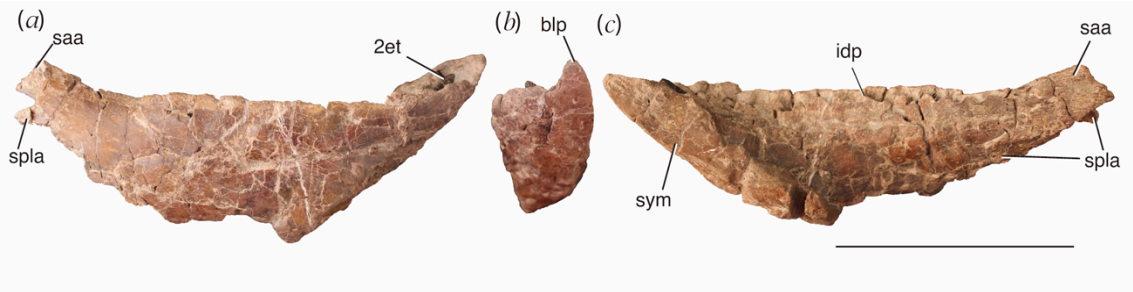

Fig. S7. Right dentary (MPE-PV 3302-3). (***a***) Lateral view. (***b***) Anterior view. (***c***) Medial view. Scale bar, 10 cm. blp, beak like process; idp, interdental plate; saa, surangular articulation; spla, splenial articulation; sym, symphysis; 2et, second erupted tooth.

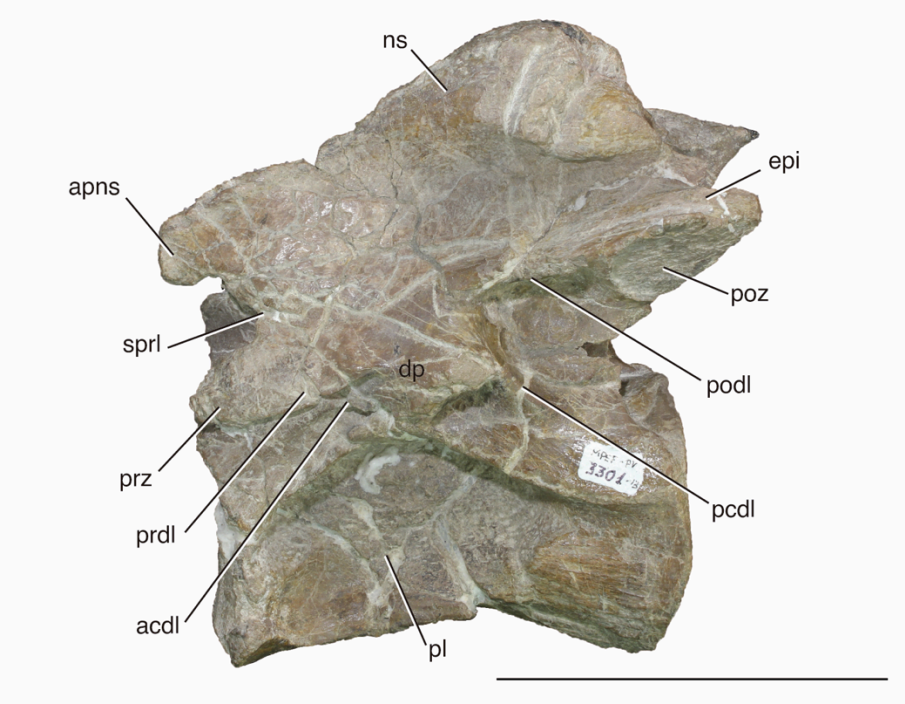

Fig. S8. Axis (MPEF-PV 3301-13) in left lateral view. Scale bar, 10 cm. acdl, anterior centrodiapophyseal lamina; apns, anterior process of the neural spine; dp, diapophysis; epi, epipophysis; ns, neural spine; pcdl, posterior centrodiapophyseal lamina; pl, pleurocoel; podl, postzygodiapophyseal lamina; poz, postzygapophysis; prdl, prezygodiapophyseal lamina; prz, prezygapophysis; sprl, spinoprezygapophyseal lamina.

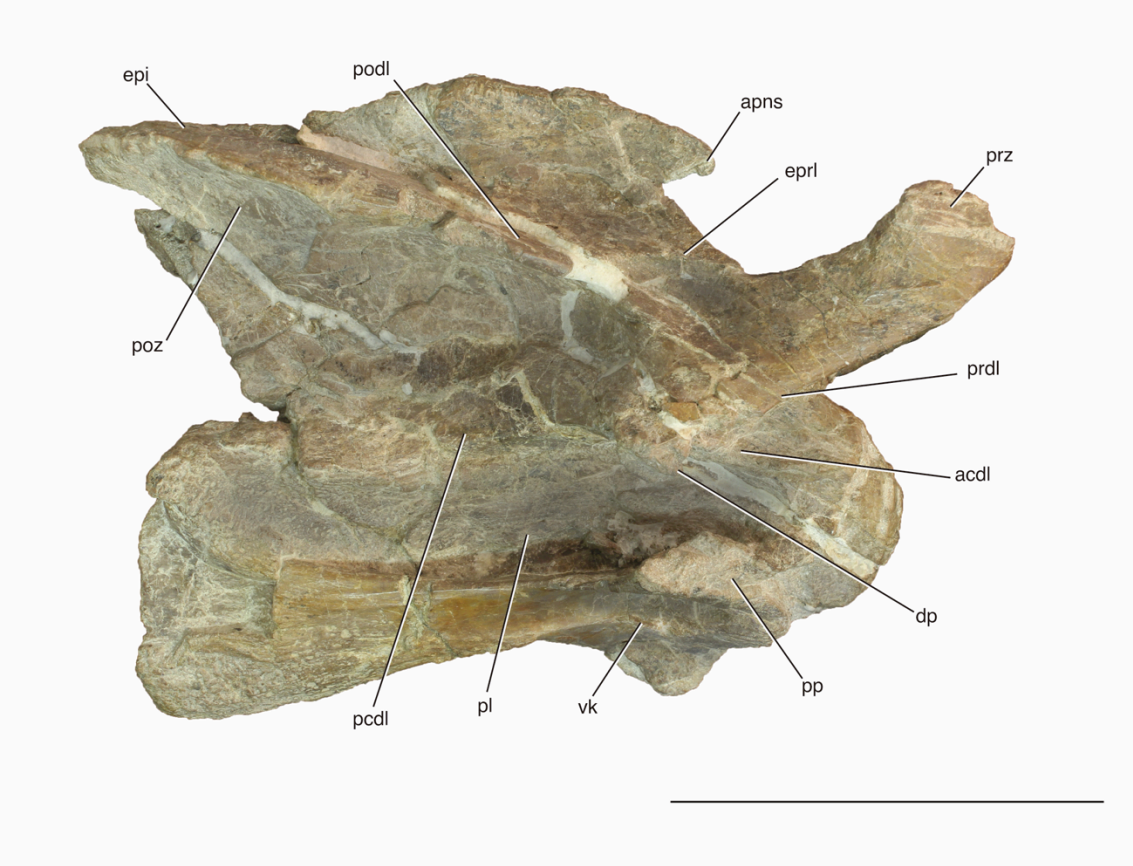

Fig. S9. Third cervical vertebra (MPEF-PV 3301-12) in right lateral view. Scale bar, 10 cm. acdl, anterior centrodiapophyseal lamina; apns, anterior process of the neural spine; dp, diapophysis; epi, epipophysis; eprl, epipophyseal-prezygapophyseal lamina; ns, neural spine; pcdl, posterior centrodiapophyseal lamina; pl, pleurocoel; podl, postzygodiapophyseal lamina; poz, postzygapophysis; pp, parapophysis; prdl, prezygodiapophyseal lamina; prz, prezygapophysis; vk, ventral keel.

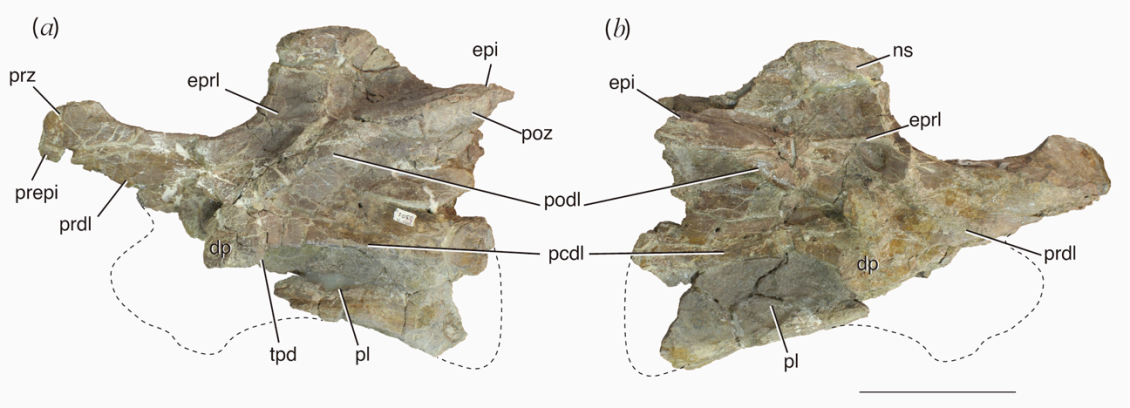

Fig. S10. Sixth cervical vertebra (MPEF-PV 3301-15). (***a***) Left lateral view. (***b***) Right lateral view. Scale bar, 10 cm. dp, diapophysis; epi, epipophysis; eprl, epipophyseal-prezygapophyseal lamina; ns, neural spine; pcdl, posterior centrodiapophyseal lamina; pl, pleurocoel; podl, postzygodiapophyseal lamina; poz, postzygapophysis; prdl, prezygodiapophyseal lamina; prepi, pre-epipophysis; prz, prezygapophysis; tpd, triangular process of the diapophysis.

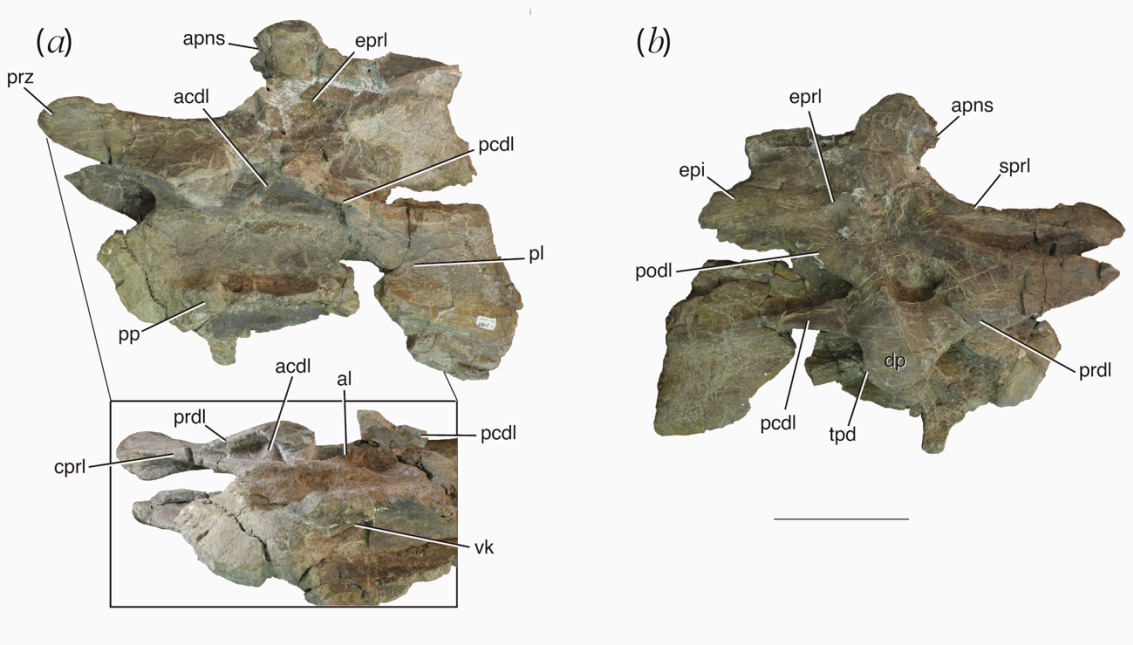

Fig. S11. Seventh cervical vertebra (MPEF-PV 3301-16). (***a***) Left lateral and anteroventral views. (***b***) Right lateral view. Scale bar, 10 cm. acdl, anterior centrodiapophyseal lamina; al, accessory lamina; apns, anterior process of the neural spine; dp, diapophysis; epi, epipophysis; eprl, epipophyseal-prezygapophyseal lamina; ns, neural spine; pcdl, posterior centrodiapophyseal lamina; pl, pleurocoel; podl, postzygodiapophyseal lamina; poz, postzygapophysis; pp, parapophysis; prdl, prezygodiapophyseal lamina; prz, prezygapophysis; sprl, spinoprezygapophyseal lamina; tpd, triangular process of the diapophysis; vk, ventral keel.

Fig. S12. Strict consensus of the parsimony phylogenetic analysis.

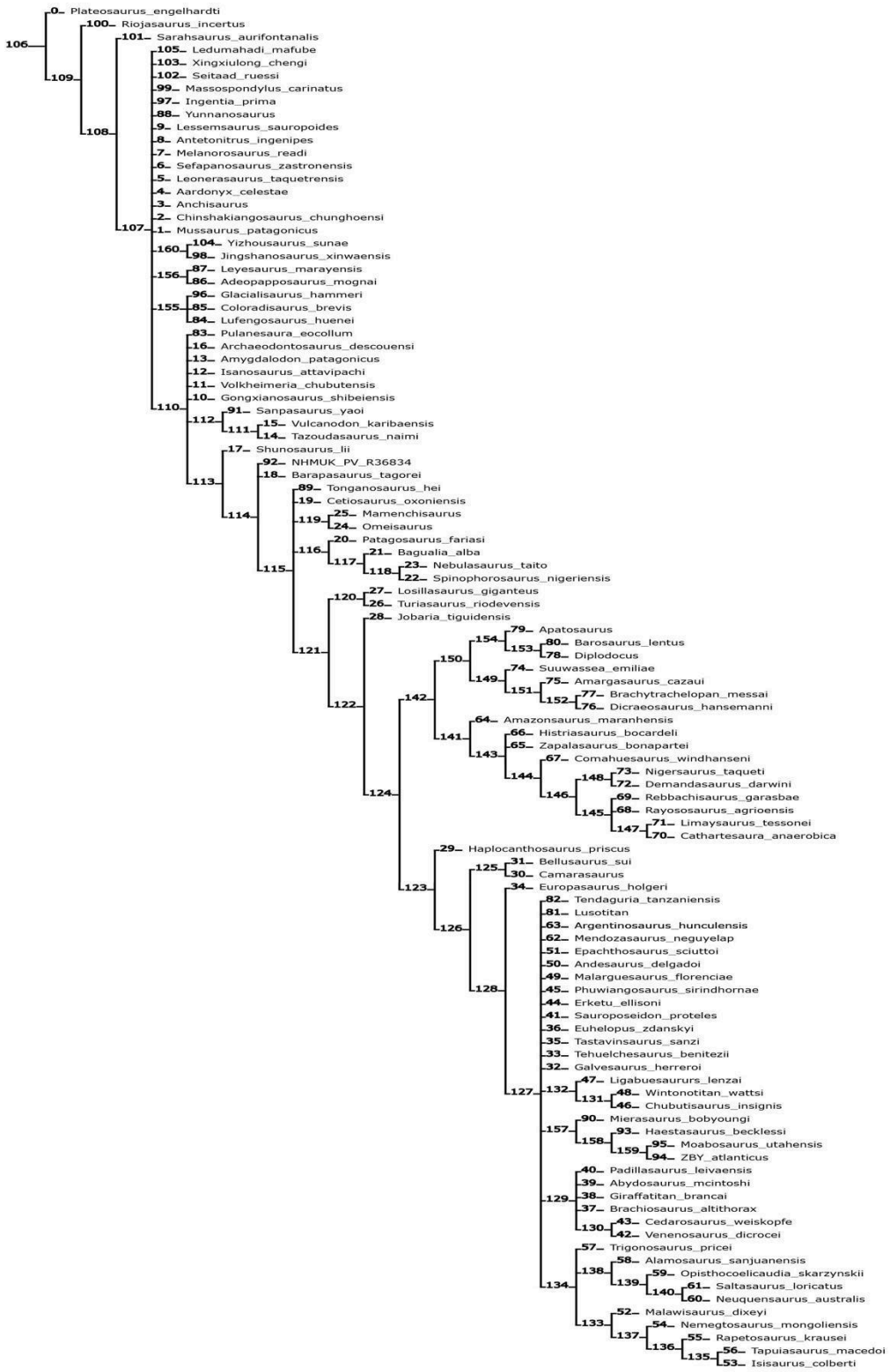
0 Plateosaurus_engelhardti
100 Riojasaurus_incertus
106
101 Sarahsaurus_aurifontanalis
105 Ledumahadi_mafube
103 Xingxiulong_chengi
102 Seitaad_ruessi
99 Massospondylus_carinatus
97 Ingentia_prima
88 Yunnanosaurus
109
9 Lessemsaurus_sauropoides
108
8 Antetonitrus_ingenipes
7 Melanorosaurus_readi
6 Sefapanosaurus_zastronensis
5 Leonerasaurus_taquetrensis
4 Aardonyx_celestae
3 Anchisaurus
2 Chinshakiangosaurus_chunghoensis
107
1 Mussaurus_patagonicus
160
104 Yizhousaurus_sunae
98 Jingshanosaurus_xinwaensis
156
87 Leyesaurus_marayensis
86 Adeopapposaurus_mognai
96 Glacialisaurus_hammeri
155
85 Coloradisaurus_brevis
84 Lufengosaurus_huenei
83 Pulanesaura_eocollum
16 Archaeodontosaurus_descouensi
13 Amygdalodon_patagonicus
12 Isanosaurus_attavipachi
11 Volkheimeria_chubutensis
10 Gongxianosaurus_shibeiensis
110
91 Sanpasaurus_yaoi
112
111
15 Vulcanodon_karibaensis
14 Tazoudasaurus_naimi
17 Shunosaurus_lii
92 NHMUK_PV_R36834
18 Barapasaurus_tagorei
113
89 Tonganosaurus_hei
19 Cetiosaurus_oxoniensis
114
119
25 Mamenchisaurus
24 Omeisaurus
20 Patagosaurus_fariasi
116
117
21 Bagualia_alba
118
23 Nebulasaurus_taito
22 Spinophorosaurus_nigeriensis
115
120
27 Losillasaurus_giganteus
26 Turiasaurus_riodevensis
28 Jobaria_tiguidensis
121
79 Apatosaurus
154
80 Barosaurus_lentus
153
78 Diplodocus
150
74 Suuwassea_emiliae
149
75 Amargasaurus_cazaui
151
77 Brachytrachelopan_messai
152
76 Dicraeosaurus_hansemanni
122
142
64 Amazonsaurus_maranhensis
66 Histriasaurus_bocardeli
141
65 Zapalasaurus_bonapartei
143
67 Comahuesaurus_windhanseni
144
73 Nigersaurus_taqueti
148
72 Demandasaurus_darwini
146
69 Rebbachisaurus_garasbae
68 Rayososaurus_agrioensis
145
147
71 Limaysaurus_tessonei
70 Cathartesaura_anaerobica
124
29 Haplocanthosaurus_priscus
125
31 Bellusaurus_sui
30 Camarasaurus
123
34 Europasaurus_holgeri
82 Tendaguria_tanzaniensis
81 Lusotitan
63 Argentinosaurus_huinculensis
62 Mendozasaurus_neguyelap
51 Epachthosaurus_sciuttoi
50 Andesaurus_delgadoi
49 Malarguesaurus_florenciae
126
128
45 Phuwiangosaurus_sirindhornae
44 Erketu_ellisoni
41 Sauroposeidon_proteles
36 Euhelopus_zdanskyi
35 Tastavinsaurus_sanzi
33 Tehuelchesaurus_benitezii
32 Galvesaurus_herreroi
47 Ligabuesaurus_lenzai
132
131
48 Wintonotitan_wattsi
46 Chubutisaurus_insignis
127
90 Mierasaurus_bobyoungi
157
158
93 Haestasaurus_becklessi
159
95 Moabosaurus_utahensis
94 ZBY_atlanticus
40 Padillasaurus_leivaensis
39 Abydosaurus_mcintoshi
129
38 Giraffatitan_brancai
37 Brachiosaurus_altithorax
130
43 Cedarosaurus_weiskopfe
42 Venenosaurus_dicrocei
57 Trigonosaurus_pricei
58 Alamosaurus_sanjuanensis
138
59 Opisthocoelicaudia_skarzynskii
139
61 Saltasaurus_loricatus
140
60 Neuquensaurus_australis
134
52 Malawisaurus_dixeyi
133
54 Nemegtosaurus_mongoliensis
137
55 Rapetosaurus_krausei
136
56 Tapuiasaurus_macedoi
135
53 Isisaurus_colberti

Fig. S13. Reduced strict consensus of the parsimony phylogenetic analysis.

Fig. S14. Bremer support values obtained in the phylogenetic analysis.

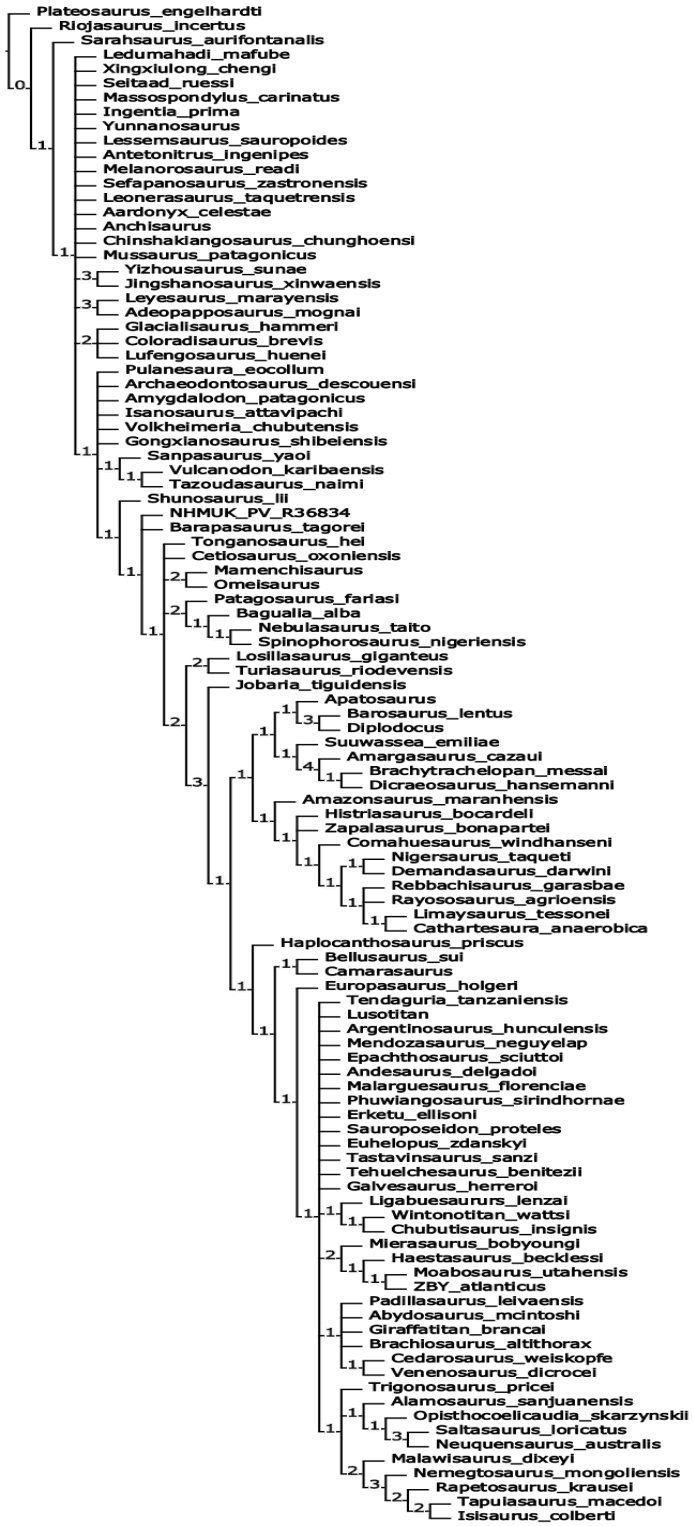

Fig. S15. Jackknife support values obtained in the phylogenetic analysis.

Fig. S16. PCRJak analysis showing jackknife support values on a reduced majority rule consensus obtained after ignoring the phylogenetically unstable taxa [see S39].

Table S1. Summary of calculated U-Pb ages and their uncertainties.

Sample	Formation	Section	Latitude (S)	Longitude (W)	$^{206}Pb/^{238}U$ date	Uncertainty (2σ)			MSWD	*n*	#
						X	*Y*	*Z*			
CA041412-2	Cañadón Asfalto	La Huinco	43°31'17.58"	69° 8'15.61"	178.07	0.21	0.25	0.31	0.46	6	8
EB041412	Cañadón Asfalto	El Bagual	43°27'36.00"	69°11'4.89"	179.17	0.12	0.16	0.25	1.1	5	5
FF022616-1	Lonco Trapial	Highway 12	43°12'25.09"	69°14'21.32"	180.330	0.068	0.11	0.22	0.60	5	5

Notes:

Latitude/Longitude relative to WGS84 datum.

X: internal (analytical) uncertainty in the absence of all external or systematic errors.

Y: incorporates the U-Pb tracer calibration error.

Z: includes *X* and *Y*, as well as the uranium decay constant errors.

MSWD: mean square of weighted deviates.

n: number of analyses included in the calculated weighted mean date, out of a total number of # analyses.

Table S2. Measurement of skull elements (in mm). Asterisk (*) indicates incomplete elements.

	Height		
Lacrimal MPEF-PV 3301-11	124		
	Proximal width		
Nasal 3301-3	70*		
	Length		
Prefrontal MPEF-PV 3301-6	90		
	Length	Width	
Frontals MPEF-PV 3301-3	80	185	
	Proximal length	Height	
Postorbital MPEF-PV 3301-10	95*	125*	
	Length		
Parietal	40*		
	Length	Height	
Squamosal MPEF-PV 3301-9	70	110	
	Height	Height of the pterygoid wing	Width of the pterygoid wing
Quadrate MPEF-PV 3301-4	155	90	55
	Height	Width	
Supraoccipital MPEF-PV 3301-1	60	93	
	Height	Width	
Foramen Magnum MPEF-PV 3301-1	24	15	
	Height	Width	

Occipital condyle MPEF-PV 3301-1	41	44	
	Length		
Basipterygoid process MPEF-PV 3301-1	60		
	Length		
Cultriform process MPEF-PV 3301-1	65		
	Length	Symphysis height	
Premaxilla MPEF-PV 3305	75	73	
	Length	Height	
Maxilla MPEF-PV 3341	220*	95	
	Length	height in the midlength	height of the symphysis
Dentary MPEF-PV 3302-3	220*	57*	110
Dentary MPEF-PV 3302-1	210*	60	70*
	Length	Maximum height	
Surangular MPEF-PV 3302-2	230	70*	

Table S3. FAD and LADs or taxa used in the phylogenetic analysis

	FAD	**LAD**
Thecodontosaurus		
'Plateosaurus engelhardti'	227	201.3
Riojasaurus	227	218
'Chinshakiangosaurus chunghoensis'	201.3	199.3
'Mussaurus patagonicus'	192.7	192.6
Sarahsaurus	199.3	183.7
Xingxiulong	201.3	190.8

Ledumahadi	201.3	190.8
Seitaad	190.8	182.7
Yizhousaurus	199.3	190.8
Jingshanosaurus	201.3	190.8
Aardonyx	201.3	190.8
Coloradisaurus	227	218
Massospondylus	201.3	190.8
Ingentia	209.5	201.3
Glacialisaurus	199	182
Yunnanosaurus	201.3	190.8
Lufengosaurus	201.3	190.8
Leonerasaurus	189	188.8
Anchisaurus	201.3	190.8
Leyesaurus	201.3	190.8
Adeopapposaurus	201.3	190.8
Sefapanosaurus	208.5	190.8
Melanorosaurus	228.4	201.3
'Antetonitrus ingenipes'	201.3	190.8
'Lessemsaurus sauropoides'	228.4	209.5
Pulanesaura	201.3	190.8
'Amygdalodon patagonicus'	190.8	180
'Isanosaurus attavipachi'	208.5	174.1
'Volkheimeria chubutensis'	174.1	168.3
'Gongxianosaurus shibeiensis'	190.8	182.7
Sanpasaurus	182.7	174.1
'Vulcanodon karibaensis'	201.3	199.3
'Tazoudasaurus naimi'	190.8	174.1

NHMUK PV R36834	201.3	190.8
'Barapasaurus tagorei'	190.8	170.3
Archaeodontosaurus	168.3	166.1
'Shunosaurus lii'	161	157
'Cetiosaurus oxoniensis'	168.3	166.1
Tonganosaurus	182	174
Mamenchisaurus	163.5	152.1
Omeisaurus	161	157
'Nebulasaurus taito'	174.1	170.3
Spinophorosaurus	174.1	163.5
Bagualia	179.4	178.9
'Patagosaurus fariasi'	166.1	163.5
'Losillasaurus giganteus'	152.1	139.8
'Turiasaurus riodevensis'	152.1	139.8
'Jobaria tiguidensis'	145	130.8
'Haplocanthosaurus priscus'	157.3	145
Camarasaurus	157.3	145
'Bellusaurus sui'	162.2	159.7
'Europasaurus holgeri'	157.3	152.1
'Euhelopus zdanskyi'	130.8	113
Mierasaurus	142	124
Haestasaurus	145	132.9
ZBY	157.3	152.1
Moabosaurus	125	113
'Galvesaurus herreroi'	152.1	139.8
'Tehuelchesaurus benitezii'	157.3	145
'Tastavinsaurus sanzi'	125	113

'Brachiosaurus altithorax'	157.3	145
'Giraffatitan brancai'	157.3	145
'Abydosaurus mcintoshi'	113	93.9
'Venenosaurus dicrocei'	130.8	126.3
'Cedarosaurus weiskopfe'	130.8	126.3
'Padillasaurus leivaensis'	129.4	125
'Sauroposeidon proteles'	113	100.5
'Erketu ellisoni'	93.9	86.3
'Phuwiangosaurus sirindhornae'	130.8	113
'Ligabuesaururs lenzai'	113	100.5
'Chubutisaurus insignis'	126.3	113
'Wintonotitan wattsi'	110	91
'Malarguesaurus florenciae'	91	87
'Andesaurus delgadoi'	100.5	93.9
'Epachthosaurus sciuttoi'	100.5	93.9
'Malawisaurus dixeyi'	126.3	113
'Isisaurus colberti'	72.1	66
'Nemegtosaurus mongoliensis'	72.1	66
'Rapetosaurus krausei'	72.1	66
'Tapuiasaurus macedoi'	126.3	113
'Trigonosaurus pricei'	72.1	66
'Alamosaurus sanjuanensis'	83.6	66
'Opisthocoelicaudia skarzynskii'	83.6	66
'Neuquensaurus australis'	83.6	72.1
'Saltasaurus loricatus'	72.1	66
'Mendozasaurus neguyelap'	89.8	86.3
'Argentinosaurus hunculensis'	113	93.9

'Amazonsaurus maranhensis'	125	100.5
'Zapalasaurus bonapartei'	130.8	113
'Histriasaurus bocardeli'	133.9	126.3
'Comahuesaurus windhanseni'	126.3	113
'Rayososaurus agrioensis'	100.5	93.9
'Rebbachisaurus garasbae'	100.5	93.9
'Cathartesaura anaerobica'	100.5	93.9
'Limaysaurus tessonei'	100.5	93.9
'Demandasaurus darwini'	130.8	113
'Nigersaurus taqueti'	126.3	93.9
'Suuwassea emiliae'	157.3	145
'Dicraeosaurus hansemanni'	157.3	145
'Amargasaurus cazaui'	130.8	113
'Brachytrachelopan messai'	152.1	145
Diplodocus	157.3	145
Apatosaurus	157.3	145
'Barosaurus lentus'	157.3	145
Lusotitan	157.3	145
'Tendaguria tanzaniensis'	157.3	145

Table S4. Body mass of taxa in Figure 3. Mean and estimated errors in kg. Data taken from previous works [S30, S31].

Taxon	Mean	Error (±)	Log(mass)
Eoraptor lunensis	1.70E+01	±4.3	1.230448921
Pampadromaeus barberenai	8.50E+00	±2.16	0.931647963
Saturnalia tupiniquim	1.10E+01	±2.79	1.027219237
Chromogisaurus novasi	1.30E+01	±3.3	1.115704417
Pantydraco caducus	1.20E+00	±0.30	0.065508027
Thecodontosaurus antiquus	3.00E+01	±7.62	1.472756449
Efraasia minor	3.70E+01	±9.39	1.571058621
Plateosauravus cullingworthi	1.30E+03	±330.2	3.127571997
Ruehleia bedheimensis	1.10E+03	±279.4	3.058512304
Plateosaurus engelhardti	9.20E+02	±233.68	2.962591854
Plateosaurus erlenbergiensis	4.60E+02	±116.84	2.658869592

Riojasaurus incertus	1.10E+03	±279.4	3.058512304
Eucnemesaurus fortis	6.90E+02	±175.26	2.838303382
Sarahsaurus aurifontanalis	1.00E+02	±25.4	2.000842389
Massospondylus carinatus	4.90E+02	±124.46	2.688186228
Adeopapposaurus mognai	4.40E+01	±11.17	1.642570454
Lufengosaurus huenei	2.30E+03	±584.2	3.353918533
Coloradisaurus brevis	5.80E+02	±147.32	2.759667845
Jingshanosaurus xinwaensis	2.90E+03	±736-6	3.465021912
Yunnanosaurus huangi	4.30E+02	±109.22	2.637153531
Anchisaurus polyzelus	1.40E+02	±35.56	2.1384858
Mussaurus patagonicus	1.02E+03	±259.08	3.130333768
Aardonyx celestae	1.40E+03	±355.6	3.146128036
Melanorosaurus readi	1.40E+03	±355.6	3.159266331
Lessemsaurus sauropoides	6.00E+03	±1524	3.245529037

Ledumahadi	1.20E+04	±3048	4.079181246
Antetonitrus igenipes	5.60E+03	±1422.4	3.751259344
Lamplughsaura dharmarensis	1.00E+03	±254	3.006466042
Tazoudasaurus naimi	1.01E+04	±2565.4	4.004321374
Vulcanodon karibaensis	9.80E+03	±2489.2	3.98999997
Shunosaurus lii	6.70E+03	±1701.8	3.824201093
Bagualia	1.00E+04	±2540	4
Cetiosaurus oxoniensis	2.70E+04	±6858	4.435444427
Klamelisaurus gobiensis	1.10E+04	±2794	4.042228524
Chuanjiesaurus anaensis	1.60E+04	±4064	4.211820894
Mamenchisaurus youngi	6.20E+03	±1574.8	3.795215358
Mamenchisaurus constructus	1.80E+04	±4572	4.24529491
Mamenchisaurus jingyanensis	8.70E+03	±2209.8	3.939519253
Yuanmousaurus jiangyiensis	7.80E+03	±1981.2	3.891892703
Cetiosauriscus stewarti	1.60E+04	±4064	4.192617981

Omeisaurus tianfuensis	1.60E+04	±4064	4.197476556
Omeisaurus maoianus	7.80E+03	±1981.2	3.891892703
Omeisaurus junghsiensis	8.90E+03	±2260.6	3.949446182
Ferganasaurus verzilini	8.80E+03	±2235.2	3.944725434
Turiasaurus riodevensis	5.10E+04	±12954	4.706917003
Jobaria tiguidensis	1.40E+04	±3556	4.133903915
Lapparentosaurus madagascariensis	1.40E+03	±3556	3.144092455
Atlasaurus imelakei	2.60E+04	±6604	4.414695029
Limaysaurus tessonei	1.20E+04	±3048	4.064284271
Comahuesaurus windhauseni	1.20E+04	±3048	4.091015648
Dicraeosaurus hansemanni	1.00E+04	±2540	4.007032713
Amargasaurus cazaui	1.10E+04	±2794	4.030887073
Apatosaurus ajax	3.30E+04	±8382	4.521991235

Apatosaurus excelsus	3.10E+04	±7874	4.484896426
Apatosaurus parvus	2.40E+04	±6096	4.385195037
Apatosaurus louisae	4.10E+04	±10414	4.615620985
Tornieria africana	1.20E+04	±3048	4.090055885
Barosaurus lentus	1.30E+04	±3302	4.119372252
Diplodocus hayi	1.60E+04	±4064	4.213067637
Diplodocus carnegii	1.40E+04	±3556	4.139906962
Diplodocus longus	1.50E+04	±3810	4.170645384
Lourinhasaurus alenquerensis	3.10E+04	±7874	4.485793162
Camarasaurus lentus	2.60E+04	±6604	4.407492879
Camarasaurus grandis	1.80E+04	±4572	4.25946399
Camarasaurus supremus	2.90E+04	±7366	4.465382851
Janenschia robusta	1.40E+04	±3556	4.135106941
Tehuelchesaurus benitezii	4.10E+04	±10414	4.615620985

Fukuititan nipponensis	6.80E+03	±1727.2	3.833754084
Pleurocoelus nanus	5.20E+02	±132.08	2.715872958
Europasaurus holgeri	1.00E+03	±254	3.019210447
Brachiosaurus sp.	5.60E+04	±14224	4.750160575
"*Bothriospondylus*" from France	1.50E+04	±3810	4.165145259
Giraffatitan brancai	3.40E+04	±8636	4.531519061
Cedarosaurus weiskopfae	1.50E+04	±3810	4.184569781
Euhelopus zdanskyi	5.90E+03	±1498.6	3.772625428
Phuwiangosaurus sirindhornae	9.70E+03	±2463.8	3.984599376
Diamantinasaurus matildae	2.30E+04	±5842	4.363175286
Sauroposeidon proteles	1.20E+04	±3048	4.094752751
Chubutisaurus insignis	2.90E+04	±7366	4.464995907
Ligabuesaurus leanzai	2.00E+04	±5080	4.310370607

Futalognkosaurus dukei	3.80E+04	±9652	4.581364436
Epachthosaurus sciuttoi	1.30E+04	±3302	4.113264804
Dreadnoughtus schrani	5.93E+04	±15062.2	4.579783597
Bonatitan reigi	1.00E+03	±254	3.006901023
Malawisaurus dixeyi	7.00E+03	±1778	3.842289755
Ampelosaurus atacis	9.40E+03	±2387.6	3.973127854
Magyarosaurus dacus	7.50E+02	±190.5	2.872822843
Lirainosaurus astibiae	1.80E+03	±457.2	3.256090401
Rinconsaurus caudamirus	4.10E+03	±1041.4	3.610625985
Jainosaurus septentrionalis	1.20E+04	±3048	4.077211985
Antarctosaurus wichmannianus	2.30E+04	±5842	4.355234918
Antarctosaurus brasilensis	2.00E+04	±5080	4.307397005
Alamosaurus sanjuanensis	3.50E+04	±8890	4.546095946
Opisthocoelicaudia skarzynskii	2.50E+04	±6350	4.40514295
Neuquensaurus australis	6.10E+03	±1549.4	3.783414444

Saltasaurus loricatus	5.80E+03	±1473.2	3.761168144
Rapetosaurus krausei	1.60E+03	±406.4	3.216316249

Dataset S1. Phylogenetic data matrix (plain text file, formatted for TNT)

Dataset S2. U-Pb data in spreadsheet (Excel file)

Both datasets have been deposited in Dryad under the following

DOI: 10.5061/dryad.x0k6djhh7

References

S1. Cúneo R, Ramezani J, Scasso R, Pol D, Escapa I, Zavattieri AM, Bowring SA. 2013. High-precision U-Pb geochronology and a new chronostratigraphy for the Cañadón Asfalto Basin, Chubut, central Patagonia: Implications form terrestrial faunal and floral evolution in Jurassic. *Gondwana Research* **24**, 1267–1275. (doi: 10.1016/j.gr.2013.01.010)

S2. Ramezani J, Hoke GD, Fastovsky DE, Bowring SA, Therrien F, Dworkin SI, Atchley SC, Nordt LC. 2011. High-precision U-Pb zircon geochronology of the Late Triassic Chinle Formation, Petrified Forest National Park (Arizona, USA): Temporal constraints on the early evolution of dinosaurs. *Geological Society of America Bulletin* **123**, 2142–2159.

S3. Mattinson JM. 2005. Zircon U/Pb chemical abrasion (CA-TIMS) method; combined annealing and multi-step partial dissolution analysis for improved precision and accuracy of zircon ages. *Chemical Geology* **220**, 47–66.

S4. Condon DJ, Schoene B, McLean NM, Bowring SA, Parrish RR. 2015. Metrology and traceability of U-Pb isotope dilution geochronology (EARTHTIME Tracer Calibration Part I). *Geochimica Et Cosmochimica Acta* **164**, 464–480.

S5. McLean NM, Condon DJ, Schoene B, Bowring SA. 2015. Evaluating uncertainties in the calibration of isotopic reference materials and multi-element isotopic tracers (EARTHTIME Tracer Calibration Part II). *Geochimica Et Cosmochimica Acta* **164**, 481–501.

S6. McLean NM, Bowring JF, Bowring SA. 2011. An algorithm for U-Pb isotope dilution data reduction and uncertainty propagation. *Geochemistry Geophysics Geosystems* **12**.

S7. Bowring JF, McLean NM, Bowring SA. 2011. Engineering cyber infrastructure for U-Pb geochronology: Tripoli and U-Pb_Redux. *Geochemistry Geophysics Geosystems* **12**.

S8. Jaffey AH, Flynn KF, Glendenin LE, Bentley WC, Essling AM. 1971. Precision Measurement of Half-Lives and Specific Activities of 235U and 238U. *Physical Review C* **4**, 1889–1906.

S9. Pol D., Powell JE. 2007. Skull anatomy of Mussaurus patagonicus (Dinosauria: Sauropodomorpha) from the Late Triassic of Patagonia. *Historical Biology* **19**:125–144.

S10. Yates AM. 2007. The first complete skull of the Triassic dinosaur *Melanorosaurus* Haughton (Sauropodomorpha: Anchisauria). *Special pappers in Paleontology* **77**:9-55.

S11. Barrett PM, Upchurch P, Wang X-L. 2005. Cranial osteology of *Lufengosaurus huenei* Young (Dinosauria: Prosauropoda) from the Lower Jurassic of Yunnan, People's Republic of China. *J Vert Paleontol* **25**:806–822.

S12. Chatterjee S, Zheng Z. 2002. Cranial anatomy of *Shunosaurus*, a basal sauropod dinosaur from the Middle Jurassic of China. *Zoological Journal of the Linnean Society* **136**:145-169.

S13. Moore AJ, Upchurch P, Barret PM, Clark JM, Xing X. 2020. Osteology of *Klamelisaurus gobiensis* (Dinosauria, Eusauropoda) and the evolutionary history of Middle-Late Jurassic Chinese sauropods. *Journal of Systematic Paleontology*, 1-95.

S14. Carballido JL, Sander PM. 2014. Postcranial axial skeleton of *Europasaurus holgeri* (Dinosauria, Sauropoda) from the Upper Jurassic of Germany: implications for sauropod ontogeny and phylogenetic relationships of basal Macronaria. *Journal of Systematic Palaeontology* **12**: 335–387.

S15. Wilson JA, D'emic MD, Ikejiri T, Moacdieh EM, Whitlock JA. 2011. A Nomenclature for Vertebral Fossae in Sauropods and Other Saurischian Dinosaurs. *PLoS ONE* **6**:e17114.

S16. Britt BB, Scheetz RD, Whiting MF, Wilhite DR. 2017. *Moabosaurus utahensis* n. gen., n. sp., a new sauropod from the Early Cretaceous (Aptian) of North America. *Contributions from the Museum of paleontology*, University of Michigan **32**: 189–243.

S17. Wilson JA, Sereno PC. 1998. Early evolution and higher-level phylogeny of sauropod dinosaurs. *Society of Vertebrate Paleontology*, Memoir 5, 1–68.

S18. Upchurch P. 1998. The phylogenetic relationships of sauropod dinosaurs. *Zoological Journal of the Linnean Society* **124**:43–103. (doi 10.1111/j.1096 3642.1998.tb00569.x)

S19. González Riga BJ, Previtera E, Pirrone C. 2009. *Malarguesaurus florenciae* gen. Et sp. nov., a new titanosauriform (Dinosauria, Sauropoda) from the Upper Cretaceous of Mendoza, Argentina. *Cretaceous Research* **30**:135-148.

S20. Barrett PM, Upchurch P. 2005. Sauropodomorph diversity through time: paleoecological and macroevolutionary implications. In The Sauropods (eds K Curry Rogers, JA Wilson) pp 125–152. Berkeley, CA: University of California Press.

S21. Yates AM. 2004. *Anchisaurus polyzelus* (Hitchcock): the smallest known sauropod dinosaur and the evolution of gigantism amongst sauropodomorph dinosaurs. *Postilla* **230**, 1–58.

S22. Carballido JL, Pol D. 2010. The dentition of *Amygdalodon patagonicus* (Dinosauria: Sauropoda) and the dental evolution in basal sauropods. *Comptes Rendus Palevol* **9**:83-93.

S23. Wilson JA. 2005. Overview of sauropod phylogeny and evolution. In The Sauropods (eds K Curry Rogers, JA Wilson) pp 15–49. Berkeley, CA: University of California Press.

S24. Holwerda, FM, Pol D, Rauhut OWM. 2015. Using dental enamel wrinkling to define sauropod tooth morphotypes from the Cañadón Asfalto Formation, Patagonia, Argentina. *Plos One* **10**: e0118100.

S25. Carballido JL, Holwerda FM, Pol D, Rauhut OWM. 2017. An Early Jurassic sauropod tooth from Patagonia (Cañadón Asfalto Formation): Implications for sauropod diversity. *Publicación Electrónica de la Asociación Paleontológica Argentina* **17**, 50-57.

S26. Allain R, Aquesbi N. 2008. Anatomy and phylogenetic relationships of *Tazoudasaurus naimi* (Dinosauria, Sauropoda) from the late Early Jurassic of Morocco. *Geodiversitas* **30**, 345–424.

S27. Carballido JL, Pol D, Otero A, Cerda IA, Salgado L, Garrido AC, Ramezani J, Cúneo NR, Krause JM. 2017. A new giant titanosaurs sheds light on body mass evolution among sauropod dinosaurs. *Proceedings of the Royal Society B: Biological Sciences* **284**, 20171219.

S28. Becerra MG, Gomez KL, Pol D. 2017. A sauropodomorph tooth increases the diversity of dental morphotypes in the Cañadón Asfalto Formation (Early–Middle Jurassic) of Patagonia. *Comptes Rendus Palevol* **16**, 832–840. (doi: 10.1016/j.crpv.2017.08.00

S29. Wilson JA. 2002. Sauropod dinosaur phylogeny: critique and cladistic analysis. *Zoological Journal of the Linnean Society* **136**, 215–275.

S30. McPhee BW, Benson RBJ, Botha-Brink J, Bordy EM, Choiniere JN. 2018. A giant dinosaur from the earliest Jurassic of South Africa and the transition to quadrupedality in early sauropodomorphs. *Current Biology* **28**, 1–9.

S31. Apaldetti C, Martínez RN, Cerda IA, Pol D, Alcober O. 2018. An early trend towards gigantism in Triassic sauropodomorph dinosaurs. *Nature Ecology & Evolution* **2**, 1227–1232.

S32. McPhee BW, Bordy EM, Sciscio L, Choiniere JN. 2017. The sauropodomorph biostratigraphy of the Elliot Formation of southern Africa: tracking of Sauropodomorpha across Triassic-Jurassic boundary. *Acta Palaeontologica Polonica* **62**, 441–465.

S33. Pol D, Garrido A, Cerda IA. 2011. A new sauropodomorph dinosaur from the Early Jurassic of Patagonia and the origin and evolution of the sauropod-type sacrum. *PloS ONE* **6**, e14572.

S34. LI K, Yang C-Y, Liu J, Wang Z-X. 2010. A new sauropod from the lower jurassic of huili, sichuan, china. *Vertebrata Palasiatica* **3**, 3.

S35. Zhang QN, You HL, Wang T, Chatterjee S. 2018. A new sauropodiform dinosaur with a ‘sauropodan’skull from the Lower Jurassic Lufeng Formation of Yunnan Province, China. *Scientific reports*, **8**, 1–12.

S36. McPhee BW, Upchurch P, Mannion PD, Sullivan C, Butler RJ, Barret PM. 2016. A revision of *Sanpasaurus yaoi* Young, 1944 from the Early Jurassic of China, and its relevance to the early evolution of Sauropoda (Dinosauria). *PeerJ* **4**:e2578.

S37. Nicholl CSC, Mannion PD, Barret PM. 2018. Sauropod dinosaur remains from a new Early Jurassic locality in the Central High Atlas of Morocco. *Acta Paleontologica Polónica* **63**, 147–157.

S38. Goloboff PA, Catalano SA. 2016. TNT version 1.5, including a full implementation of phylogenetic morphometrics. *Cladistics* **32**, 221–238.

S39. Pol D, Goloboff PA. 2020. The impact of unstable taxa in coelurosaurian phylogeny and resampling support measures for parsimony analyses. Bulletin of the American Museum of Natural History 440: 97–115.

S40. Carballido JL, Scheil M, Knötschke N, Sander PM. 2019. The appendicular skeleton of the dwarf macronarian sauropod *Europasaurus holgeri* from the Late Jurassic of Germany and a re-evaluation of its systematic affinities. *Journal of Systematic Palaeontology*, DOI: 10.1080/14772019.2019.1683770

S41. Wilkinson M, Thorley JL, Upchurch P. 2000. A Chain Is No Stronger than Its Weakest Link: Double Decay Analysis of Phylogenetic Hypotheses. Systematic Biology 49: 754–776.

S42. Goloboff PA. 1993. Estimating character weights during tree search. *Cladistics* **9**, 83–91.

S43. Goloboff PA. 2014. Extended implied weighting. *Cladistics* **30**, 260–272.

S44. Ronquist F, Teslenko M, Van Der Mark P, Ayres DL, Darling A, Hohna S, Larget B, Liu L, Suchard MA, Huelsenbeck JP. 2012. MrBayes 3.2: Efficient Bayesian Phylogenetic Inference and Model Choice Across a Large Model Space. *Systematic Biology* **61**, 539–542.

S45. Whitlock JA. 2011. A phylogenetic analysis of Diplodocoidea (Saurischia: Sauropoda). *Zoological Journal of the Linnean Society* **161**: 872–915.

S46. Zaher H, Pol D, Carvalho AB, Nascimento PM, Riccomini C, et al. 2011. A Complete Skull of an Early Cretaceous Sauropod and the Evolution of Advanced Titanosaurians. *PLoS ONE* **6**(2): e16663. (doi:10.1371/journal.pone.0016663)

S47. Carballido JL, Salgado L, Pol D, Canudo JI, Garrido A. 2012. A new basal rebbachisaurid (Sauropoda, Diplodocoidea) from the Early Cretaceous of the Neuquén Basin; evolution and biogeography of the group. *Hist. Biol*. **24**, 631–654. (doi:10.1080/08912963.2012.672416)

S48. Upchurch P, Barrett PM, Dodson P. 2004 The Dinosauria. In The Dinosauria (eds DB Weishampel, P Dodson, H Osmólska), pp. 259–322. Berkeley, CA: University of California Press.

S49. Curry Rogers K. 2005. Titanosauria, a phylogenetic overview. In The Sauropods (eds K Curry Rogers, JA Wilson), 50-103 pp. Berkeley, CA: University of California Press.

S50. Mannion P, Upchurch P, Barnes RN, Mateus O. 2013 Osteology of the Late Jurassic Portuguese sauropod dinosaur *Lusotitan atalaiensis* (Macronaria) and the evolutionary history of basal titanosauriforms. *Zool. J. Linn. Soc*. **168**: 98–206. (doi:10.1111/zoj. 12029)

S51. Salgado L, Coria RA, Calvo JO. 1997. Evolution of titanosaurid sauropods. I: Phylogenetic analysis based on the postcranial evidence. *Ameghiniana* **34**:3–32.

S52. Harris JD. 2006. The significance of *Suuwassea emilieae* (Dinosauria: Sauropoda) for Flagellicaudatan intrarelationships and evolution. *Journal of Systematic Palaeontology* **4**:185–198.

S53. Sereno PC, Wilson JA, Witmer LM, Whitlock JA, Maga A, Ide O, Rowe TA. 2007. Structural extremes in a Cretaceous dinosaur. *PLoS ONE* **2**: e1230.

S54. Carballido JL, Pol D, Cerda L, Salgado L. 2011. The Osteology of *Chubutisaurus insignis* Del Corro, 1975 (Dinosauria: Neosauropoda) from the "Middle" Cretaceous of Central Patagonia, Argentina. *Journal of Vertebrate Paleontology* **31**:93-110.

S55. González Riga BJ, Previtera E, Pirrone C. 2009. *Malarguesaurus florenciae* gen. Et sp. nov., a new titanosauriform (Dinosauria, Sauropoda) from the Upper Cretaceous of Mendoza, Argentina. *Cretaceous Research* **30**:135-148.

S56. Upchurch P, Barrett PM, Galton PM. 2007. A phylogenetic analysis of basal sauropodomorph relationships: implications for the origin of sauropod dinosaurs. In Evolution and Palaeobiology of Early Sauropodomorph dinosaurs (eds. PM Barrett, DJ Batten) Volume **77**, 57-90 pp.

S57. Mannion PD. 2009. A rebbachisaurid sauropod from the Lower Cretaceous of the Isle of Wight, England. *Cretaceous Research* **30**:521-526.

S58. Mannion PD, Upchurch P, Mateus O, Barnes R, Jones MEH. 2012 New information on the anatomy and systematic position of *Dinheirosaurus lourinhanensis* (Sauropoda: Diplodocoidea) from the Late Jurassic of Portugal, with a review of European diplodocoids. *Journal of Systematic Palaeontology* **19**:5621–551.

S59. Upchurch P. 1998. The phylogenetic relationships of sauropod dinosaurs. *Zoological Journal of the Linnean Society* **124**:43–103. (doi 10.1111/j.1096 3642.1998.tb00569.x)

S60. D'Emic MD. 2012. The early evolution of titanosauriform sauropod dinosaurs. Zoological Journal of the Linnean Society 166: 624–671.

S61. Xing L, Miyashita T, Currie PJ, You H, Zhang J, Dong Z. 2015. A new basal eusauropod from the Middle Jurassic of Yunnan, China, and faunal compositions and transitions of Asian sauropodomorph dinosaurs. *Acta Palaeontologica Polonica* **60** (1): 145–154.

S62. Remes K, Ortega F, Fierro I, Joger U, Kosma R. 2009. A New Basal Sauropod Dinosaur from the Middle Jurassic of Niger and the Early Evolution of Sauropoda. *PLoS ONE* **4**(9): e6924.

S63. Tschopp E, Mateus O, Benson RBJ. 2015. A specimen level phylogenetic analysis and taxonomic revision of Diplodocidae (Dinosauria, Sauropoda). *PeerJ* **3**: e857.

S64. McPhee BW, Choiniere JN. 2018. The osteology of *Pulanesaura eocollum*: implications for the inclusivity of Sauropoda (Dinosauria). *Zoological Journal of the Linnean Society* **182:**830–861. (doi:10.1093/zoolinnean/zlx074/4561573)

S65. Cooper MR. 1984. A reassessment of *Vulcanodon karibaensis* Raath (Dinosauria: Saurischia) and the origin of the Sauropoda. *Palaeontologia Africana* **25**: 203–231.